*Os*r40g3 imparts salinity tolerance by regulating GF14e-mediated modulation of gibberellin metabolism to activate expansin protein, EG45 in rice

Chandan Roy[1], Salman Sahid[1,2], Riddhi Datta[2*], Soumitra Paul[1*]

[1] Department of Botany, University of Calcutta, 35 Ballygunge Circular Road, Kolkata-700019, West Bengal, India

[2] Department of Botany, Dr. A.P.J. Abdul Kalam Government College, Plot BA-1, Action Area-1, Newtown, Rajarhat, Kolkata-700156, West Bengal, India

*****Authors for correspondence:

Email: riddhi.bot@gmail.com, psoumitra@ymail.com; Telephone No: +919433084074, +919748605305; Fax No: +9133 2461 4849

Short title: *Os*r40g3-*Os*GF14e-*Os*EG45 module regulates salt tolerance in rice

Abstract

While the role of R40 family of lectin proteins in osmotic stress was already reported, their mechanism of stress tolerance still remained elusive. Among them, the expression of *Osr40g3* was most strongly induced in response to salinity. Here, we explored the mechanism of *Osr40g3*-mediated salinity tolerance in rice. The overexpression of *Osr40g3* under control of a constitutive promoter significantly improved salinity tolerance but displayed pollen sterility and impaired seed development. The gene further displayed precise tissue-specific expression which was essential for proper seed development in rice. In salinity-stressed leaves, *Os*r40g3 interacted with *Os*EG45 leading to salinity tolerance. Overexpression of *OsEG45* significantly improved salinity tolerance while the *OsEG45* silencing lines displayed severe sensitivity thus confirming its role in imparting salinity tolerance. On the other hand, the constitutive overexpression of *Os*r40g3 led to its interaction with *Os*GF14e in stamens reducing its protein stability. This interaction further interfered with gibberellic acid (GA) metabolism thus leading to pollen sterility. The *OsGF14e* silencing lines also failed to set seeds and displayed diminished GA content thus supporting its involvement in regulating seed development. Surprisingly, these *OsGF14e* silencing lines also displayed improved salinity tolerance with higher expression of *OsEG45* while the *OsGF14e* overexpression lines displayed opposite phenotype. This altered expression of *OsEG45* was further mediated by GA levels in these transgenic lines. Together, we demonstrate that salt stress induces *Os*r40g3 which then positively regulates *Os*EG45 and negatively regulates *Os*GF14e. Inhibition of *Os*GF14e reduces GA level which further induces *OsEG45* expression thus leading to salinity tolerance in rice.

Keywords

*Os*r40g3, salinity tolerance, *Os*GF14e, OsEG45, rice

Introduction

Plants continuously face a wide range of environmental challenges including various biotic and abiotic stress factors. Fascinatingly, they can counteract most of these threats with their intricate defense signaling network and maintain growth (Muthamilasaram and Prasad, 2013). Lectins are carbohydrate-binding proteins that serve as excellent candidates in the plant signaling network. It can bind to the exogenous as well as endogenous glycan molecules to regulate stress responses in plants (Van Damme et al., 2008). The role of lectin proteins in modulating biotic stress responses has widely been reported in a variety of plant species (Ciopraga et al., 1999; Freire et al., 2002; Damico et al., 2003; Singh and Zimmerli 2013; Miyakawa et al., 2014). Emerging evidences have also highlighted their role in abiotic stress responses including heat, drought and salinity tolerance (Spadoro-Tank and Etzler, 1988; Hirano et al., 2000; Jiang et al., 2012a; He et al., 2016; Sahid et al., 2020).

The effect of salinity stress in rice growth is primarily associated with various morphological alterations like rolling of leaves, delay of panicle emergence and anthesis, spikelet desiccation, loss of pollen viability, etc. Physiological modulation in photosynthesis, mineral absorption and transpiration rate are also exhibited by different drought or salinity sensitive and tolerant rice cultivars (Golldack et al., 2014). Since hyper-salinity reduces the soil water potential, the absorption of water is hampered in plants when they are grown under the hyper saline condition. To adjust the osmotic potential and protect the cell from its harmful effect, plants accumulate different osmoprotectants and compatible solutes like proline, glycine betaine, polyols, and sugars. They also synthesize polyamines and secondary metabolites, regulate ion homeostasis, activate antioxidants including superoxide dismutase, catalase, glutathione, ascorbate, and carotenoids to survive under osmotic stress (Shehab et al., 2010; Golldack et al., 2014).These metabolic changes are regulated by an intricate signaling network involving various phytohormones (Datta et al., 2020). The role of abscisic acid (ABA) in regulating osmotic stress including salinity stress is well documented in different plant species (Verma et al., 2016). However, emerging evidences supported the role of other plant growth regulators including gibberellic acid (GA) in relieving the effect of osmotic stress (Achard et al., 2006; Verma et al., 2016). Interestingly, the lower accumulation of GA was found to be associated with higher

salinity tolerance along with reduced plant growth. For example, GA deficiency imparted drought tolerance along with reduced plant height and lodging in teff and finger millet (Plaza-Wüthrich et al., 2016). The *SPINDLY* (*SPY*) gene that encodes a negative regulator of GA was elevated in response to osmotic stress in Arabidopsis (Qin et al., 2011). On the other hand, the quadruple DELLA mutant lacking *GAI*, *RGA*, *RGL1* and *RGL2* exhibited less growth inhibition in Arabidopsis under salt stress than the wild type (WT) suggesting a DELLA-dependent growth restrain under salt stress that was also associated with lowering of the bioactive GA levels (Verma et al., 2016).

Among various stress-responsive proteins, lectins are recently gaining importance due to its diverse regulatory role against various environmental challenges (Lannoo and van Damme, 2014). The plant lectins can be classified into 12 protein families (Jiang et al., 2010). Among them, the R40 family is an interesting group of lectins that are known to play important roles in regulating drought and salinity stress (Moons et al., 1995; 1997; Paul et al., 2015). The family consists of five functional members namely, *Os*r40c1, *Os*r40c2, *Os*r40g2, *Os*r40g3 and putative *Os*r40c1, in rice (Carpentier et al., 2007; Jiang et al., 2012b). These proteins possess a ricin-B like domain that specifically recognizes galactose or N-acetyl galactosamine residues. In addition to their osmotic stress responsive activity, these R40 family proteins are also induced in response to ABA treatment (Moons et al., 1995). For example, the expression of *Osr40c1* gene is up-regulated by ABA, methyl jasmonate (MeJA) and ethephone treatments, after *Pseudomonas* infection or osmotic stress exposure in Arabidopsis (van Hove et al., 2014). Further, the protein interacts with ABA receptor PYL9 and regulates ABA-mediated stomatal closure in plants (van Hove et al., 2015). Recently, it has also been demonstrated that the overexpression of *Os*r40c1 imparts drought tolerance in rice and tobacco suggesting its drought-tolerant activity in plants (Sahid et al., 2020). The protein has, further, been demonstrated to form a multi-protein complex with the transcription factor *Os*SAP8 along with several chromatin-associated proteins to impart drought tolerance *in planta*. However, no detailed study has been undertaken so far to explore the mechanism of osmotic stress tolerance of the other R40 family proteins in rice.

In this study, we aimed to decipher the mechanism of how *Os*r40g3 protein regulates salinity tolerance in rice. It was observed that *Os*r40g3 exhibits dual function in positively regulating the

expansin protein *Os*EG45 while negatively regulating the 14-3-3 family protein, *Os*GF14e. The diminished accumulation of *Os*GF14e lowers the GA level which further induces *Os*EG45 expression, thus leading to salinity tolerance in rice.

Results

Expression of *Osr40g3* positively correlated with the salinity tolerance potential in rice

To investigate the salinity tolerance potential of selected 8 *indica* rice cultivars, the seedlings were exposed to salinity stress for 5 d (Supplementary Figure 1A). Following stress treatment, the cultivars were assessed according to standard evaluation system proposed by IRRI (2013) and several morphological parameters were recorded (Supplementary Figure 2A-D). Different biochemical parameters such as chlorophyll content, osmolyte accumulation, and hydrogen peroxide (H_2O_2) content were analyzed as well (Supplementary Figure 2E-H). Based on all these observations, the cultivars were arranged according to their salinity tolerance potential with Nonabokhra being the most tolerant while MTU1010 being the most sensitive cultivar. Next, to investigate the stress-responsive roles of the *OsR40* genes, their expression patterns were analyzed in response to salinity stress. Interestingly, it was observed that among all the 5 *OsR40* genes, the expression of *Osr40g3* was the highest under salinity stress (Supplementary Figure 3). This prompted us to explore if the expression of the *Osr40g3* gene can be correlated with the salinity tolerance potential in rice. The expression of this gene under salinity stress was indeed positively correlated with the salinity tolerance potential of the 8 rice cultivars with a 4.29-fold induction in the tolerant Nonabokhra cultivar against a 2-fold induction in the sensitive MTU1010 cultivar (Supplementary Figure 1B). This observation strongly indicated that *Osr40g3* plays a crucial role in modulating salinity tolerance in rice.

Overexpression of *Osr40g3* improved salinity tolerance but impaired seed development in rice

To validate the function of *Osr40g3* in salinity tolerance, *Osr40g3* overexpressing transgenic rice plants (ox_c lines) harboring the recombinant *35S::Osr40g3* construct were generated. The different morphological parameters like plant height, tiller numbers, shoot and root dry weight, number of panicles per plant, panicle length, number of flowers per panicle, and number of

grains per panicle were analyzed from the transgenic plants and compared with the WT and vector control (VC) plants (Figure 1A-L). In the vegetative stage, the plants displayed no phenotypic abnormalities except a reduced plant height in most of the lines. Surprisingly, at the reproductive stage, all the transgenic lines developed a shorter panicle length in comparison with the WT and VC plants. Although the number of panicles per plant did not significantly differ, most of the transgenic lines failed to produce seeds. The plant transformation was carried out in 3 independent batches and only 2 transgenic plants from the first batch and 3 plants from each of the second and third batches produced 30-35 seeds per plant.

However, when the plants were exposed to salinity stress, the transgenic plants displayed significantly improved tolerance compared with the WT and VC plants (Figure 1M). The transgenic plants maintained lower rolled leaf percentage, ion leakage, and chlorophyll degradation, but higher relative water content (RWC) over the WT and VC plants under salinity stress (Figure 1N-Q). The transgenic plants also accumulated significantly elevated levels of osmolytes as well as displayed lower lipid peroxidation and H_2O_2 accumulation (Supplementary Figure 4A-D). It was observed that the expression of the *Osr40g3* gene was significantly higher in the transgenic lines under control as well as salinity stress conditions which could account for their tolerant phenotype (Figure 1R). The amount of sodium (Na^+), potassium (K^+), and chloride (Cl^-) ions in the soil before and after salt treatment was also measured (Supplementary Table 1). The lower accumulation of Na^+ and higher K^+ level in the transgenic plants compared with the WT and VC plants during salinity stress also indicated the tolerant phenotype of the transgenic plants (Supplementary Figure 4E-F). Together, these observations suggested that *Osr40g3* overexpression could improve salinity tolerance but impaired seed development in the transgenic lines thus indicating its dual function.

Ectopic expression of *Osr40g3* improved salinity tolerance in *Arabidopsis* with no abnormality in seed development

To further confirm its dual function in a heterologous system, transgenic *Arabidopsis* plants (*ec* lines) harboring the recombinant *35S::Osr40g3* construct and ectopically expressing the *Osr40g3* gene were generated. Surprisingly, unlike in rice, the transgenic *Arabidopsis* plants displayed no abnormality in seed development. In addition, no alteration in the rosette diameter, plant height,

silique number and length, as well as seed yield per plant, was observed in the transgenic plants (Supplementary Figure 5). Yet, similar to rice, the transgenic *Arabidopsis* plants displayed significantly improved salinity tolerance which was accompanied by a higher RWC and chlorophyll content, lower Na^+ accumulation as well as an increased *Osr40g3* transcript abundance under salinity stress (Supplementary Figure 6). These observations confirmed the role of *Osr40g3* in imparting salinity tolerance in plants but indicated that its interference with the seed development is rice-specific.

Osr40g3* overexpression resulted in pollen sterility in rice but not in *Arabidopsis

To understand the differential interference of *Osr40g3* in seed development, we analyzed the floral morphology of both the rice and *Arabidopsis* transgenic plants. In rice, flowers of transgenic ox_c plants were found to be shorter than the WT and VC flowers (Supplementary Figure 7A). However, no other significant difference in the floral morphology was observed (Supplementary Figure 7B-C). Since impairment in seed development was observed, the pollen viability was tested using I_2-KI and fluorescein diacetate (FDA) staining methods. The pollen viability in all ox_c flowers was found to be drastically reduced compared with the WT and VC flowers (Supplementary Figure 7D-E). The *in vitro* pollen germination assay displayed that the most of the pollen grains from the ox_c plants failed to produce pollen tube (Supplementary Figure 7F). This observation directly supported the failure of the ox_c lines to set seeds. On contrary, the transgenic *Arabidopsis* plants showed no alteration in floral morphology, pollen viability and pollen germination supporting their perfect seed development (Supplementary Figure 8).

To check if the failure to produce seeds in the transgenic rice lines was due to pollen sterility alone, the ox_c plants were crossed with the WT plants in two separate hybridization programs. When the WT plants were emasculated and the ox_c plants were used as a male parent no seeds were produced which confirmed the pollen sterility in the transgenic plants. Interestingly, when the ox_c plants were used as a female parent and crossed with the WT plant as a male parent, hybrid seeds were developed (Supplementary Figure 9). This finding confirmed that the failure of the transgenic ox_c plants to set seed was due to its pollen sterility with no defect in its female reproductive part.

***Osr40g3* displayed a strict tissue-specific expression pattern in rice**

To understand if the *Osr40g3* gene has any specific expression pattern in rice, its expression in the WT plant was studied from different tissues at different developmental stages. For this purpose, germinating seedlings, 60 d and 120 d old plants were used and samples were collected from the root, leaf, flag leaf, flower, stamen, and seeds under milk stage, dough stage as well as mature stage as applicable. The highest expression level of the *Osr40g3* gene was observed in the leaves under all developmental stages except for germinating seedlings where a low expression level was observed in both root and shoot (Figure 2A). Intriguingly, no expression of *Osr40g3* was detected in the stamen indicating its tissue-specific expression pattern. To further validate this observation, the promoter activity of the *Osr40g3* gene was analyzed by histochemical GUS assay. The transgenic plants harboring the recombinant *Osr40g3pro::GUS* construct showed GUS expression in roots and leaves collected from different stages of development. However, in case of flower, GUS expression was observed in the pistil but not in the stamens further supporting the tissue specific expression of *Osr40g3* (Figure 2B-C).

On the other hand, since a constitutive promoter was used to overexpress the *Osr40g3* gene, the stamens of the transgenic ox_c plants showed accumulation of *Osr40g3* transcript as expected (Supplementary Figure 10A). Remarkably, the expression of *OsAGL*65, an important regulator of pollen sterility, was not detected in the flowers and stamens of the transgenic ox_c plants while it was expressed specifically in the flowers including stamens of the WT plants (Supplementary Figure 10B). This signified that the constitutive expression of the *Osr40g3* in stamens of transgenic rice induced pollen sterility. Further, the promoter activity of the *Osr40g3* gene was found to be strongly inducible under salt stress thus supporting its salinity-responsive nature (Supplementary Figure 11).

Overexpression of *Osr40g3* under control of the native promoter imparted salinity tolerance and rescued pollen sterility in rice

Since the *Osr40g3* gene followed a strict tissue-specific expression pattern, transgenic rice plants (ox_n lines) overexpressing *Osr40g3* gene under the control of the native promoter were generated. Unlike the ox_c plants, these transgenic ox_n plants displayed no phenotypic abnormalities including seed development (Figure 3A-K). Supporting this observation, the ox_n pollen grains also exhibited a similar viability and pollen germination efficiency like that of the

WT and VC plants (Supplementary Figure 12). These observations strongly suggested that the tissue-specific expression pattern of the *Osr40g3* gene is an important determinant of pollen viability and seed development in rice. Furthermore, no expression of *Osr40g3* was detected in stamens of these ox_n plants due to its tissue specific expression pattern. Concomitantly, the expression of *OsAGL65* was detected in the flowers including stamens similar to the WT plants (Supplementary Figure 13). On the other hand, these ox_n lines also displayed a significant improvement in salinity tolerance and higher *Osr40g3* transcript abundance over the WT and VC plants (Figure 3L-Q, Supplementary Figure 14).

_Os_r40g3 positively regulated _Os_EG45-like protein while hampered the stability of _Os_GF14e

To gain mechanistic insight into the function of *Osr40g3*, the interacting protein partners were identified by yeast two-hybrid (Y2H) analysis against specific cDNA libraries. To identify the protein partners of *Os*r40g3 involved in salinity tolerance, a cDNA library from salinity stressed rice plants was used for Y2H assay. The *Os*EG45-like domain containing protein (LOC4347346), a peroxisomal membrane protein, *Os*PMP22 (LOC4346360) and 60S ribosomal protein L35 (LOC4329423) were identified as interacting partners of *Os*r40g3 (Figure 4A). Out of these partners, the *Os*EG45, an expansin-like protein, was found to be up-regulated in response to salinity stress in rice (Figure 4B). On the other hand, the *Os*r40g3 protein was found to interact with three non-redundant protein partners, namely *Os*GF14e (LOC4329775), *Os*AGL20 (LOCOs03g03070), and *Os*AP2-like proteins (LOCOs0107120), when a cDNA library prepared from rice flowers was used (Figure 4C). Among these partners, the *Os*GF14e protein was reported to be associated with the regulation of seed development (Manosalva et al., 2011; Liu et al., 2016). We, therefore, confirmed the interaction of *Os*EG45 and *Os*GF14e proteins with *Os*r40g3 by bimolecular fluorescence complementation (BiFC) and co-immunoprecipitation (Co-IP) assays (Figure 4D-F). For Co-IP assay, rice calli transiently expressing *Os*r40g3-HA and *Os*EG45-cMyc/*Os*GF14e-cMyc proteins singly or in combinations were used. The protein complexes were co-immunoprecipitated using anti-HA agarose beads followed by western blot analysis using anti-HA and anti-cMyc antibodies. Western blot from total protein was used as the input.

Intriguingly, when western blot analysis was performed from total protein against anti-cMyc antibody, significantly lower band intensity was observed in case of calli co-expressing both *Os*r40g3-HA and *Os*GF14e-cMyc proteins (Figure 4F). On the other hand, no such differential band intensity was observed for the *Os*r40g3-HA and *Os*EG45-cMyc combination (Figure 4E). This prompted us to explore if the binding of *Os*r40g3 triggers *Os*GF14e protein degradation. To investigate this possibility, we treated the transfected rice calli with a proteasomal degradation inhibitor, MG132. When western blot analysis was performed using anti-cMyc antibody, lower band intensity was observed in case of calli co-transfected with *Os*r40g3 and *Os*GF14e in absence of MG132 treatment. On the other hand, no reduction in band intensity was observed when the co-transfected calli were treated with MG132 thus demonstrating proteosomal degradation of *Os*GF14e protein in presence of *Os*r40g3 (Figure 4G).

Further, it was observed that *OsGF14e* was strongly expressed in flowers including stamens of the WT plants with comparatively lower transcript abundance in leaves and roots (Supplementary Figure 15). *Osr40g3*, on contrary, followed an opposite expression pattern. This tissue-specific expression of *Osr40g3* was perturbed when the gene was constitutively overexpressed under control of the *CaMV35S* promoter. This in turn, might have interfered with the protein stability of *Os*GF14e in flowers thus leading to pollen sterility in the transgenic ox_c lines.

Although *Arabidopsis* has several GF14 orthologs, *Osr40g3* ectopic expression did not interfere with its seed development. Therefore, all the GF14 family members in *Arabidopsis* were analyzed for their interaction with *Os*r40g3 protein through Y2H analysis. Since we could not detect expression of *AtGF14-Pi* in flower, it was not included in this study. When Y2H analysis was performed using the *Os*r40g3 protein as bait and each of the *At*GF14 proteins as prey, no interaction was evident (Supplementary Figure 16). On the other hand, the expansin-like B2 precursor protein (*At*EXLB2), an ortholog of *Os*EG45, was found to interact with the *Os*r40g3 protein. The multiple sequence alignment analysis revealed a highly conserved nature of the GF14 proteins except at their C-terminal domains (Supplementary Figure 17). Consistent with this observation, it was reported earlier that the diverse C-terminal domain determines the binding specificity of the GF14 family members which supported their diverse functions (Sehnke

et al., 2006). This structural distinctiveness of *Os*GF14e presumably accounted for its binding specificity with *Os*r40g3 while its *Arabidopsis* orthologs failed to do so.

In addition, the other members of *Os*r40 family lectin proteins like *Os*r40c1, *Os*r40g2, *Os*r40c2 and putative *Os*r40c1 were also considered to identify any interaction with *Os*GF14e protein. Interestingly, none of these members except *Os*r40g3 showed interaction with *Os*GF14e (Supplementary Figure 18).

Overexpression of *OsEG45* enhanced salinity tolerance in rice

To validate the role of *Os*EG45 in regulating salinity tolerance, the *OsEG45* overexpression ($OsEG45_{ox}$) and silencing lines ($OsEG45_{si}$) were generated. The transgenic plants displayed no phenotypic abnormalities during the vegetative as well as the reproductive stages. The $OsEG45_{ox}$ and $OsEG45_{si}$ transgenic plants were subjected to salt stress for 5 d and different morphological and biochemical parameters were analyzed. The $OsEG45_{ox}$ lines exhibited significantly improved salinity tolerance with lower leaf rolling percentage, chlorophyll degradation, accumulation of Na^+ ions and lipid peroxidation, and higher RWC, K^+ content and accumulation of different osmolytes like proline and glycine betaine as compared with the WT and VC plants (Figure 5A-E, Supplementary Figure 19). On the contrary, the $OsEG45_{si}$ lines showed increased sensitivity towards salinity stress. The relative transcript abundance of *OsEG45* gene was also found to be significantly higher in the $OsEG45_{ox}$ lines while lower in the $OsEG45_{si}$ lines compared with the WT and VC plants under both control and salinity stress conditions (Figure 5F). This observation confirmed the crucial role of *OsEG45* in regulating salinity tolerance in rice.

Silencing of *OsGF14e* induced pollen sterility but improved salinity tolerance in rice

Next, to understand the role of *Os*GF14e in regulating seed development, *OsGF14e* overexpressing ($OsGF14e_{ox}$) and silencing ($OsGF14e_{si}$) transgenic rice lines were generated and different morphological parameters were recorded. Although no abnormalities were observed at the vegetative stage, the $OsGF14e_{si}$ lines failed to produce seeds while seed development in the $OsGF14e_{ox}$ lines was not compromised (Supplementary Figure 20). Among the 12 $OsGF14e_{si}$ lines generated, 4 transgenic plants produced only 18-27 seeds per plant. Pollen viability was

checked from these transgenic lines using I_2-KI and FDA staining methods. The pollen grains of *OsGF14e*$_{si}$ lines displayed severe sterility while *OsGF14e*$_{ox}$ lines showed fertile pollen grains (Supplementary Figure 21). This observation clearly demonstrated a positive role of *Os*GF14e in regulating pollen fertility in rice.

To further dissect any possible salinity responsive role of *Os*GF14e, the *OsGF14e*$_{ox}$ and *OsGF14e*$_{si}$ lines were exposed to salinity stress and different morphological and biochemical parameters were analyzed. Interestingly, the *OsGF14e*$_{si}$ lines exhibited improved salinity tolerance while the *OsGF14e*$_{ox}$ lines displayed severe sensitivity as compared with the WT and VC lines (Figure 5G). In response to salt exposure, the leaf rolling percentage, chlorophyll degradation, lipid peroxidation, and accumulation of Na^+ ions were found to be lower in the *OsGF14e*$_{si}$ lines and higher in the *OsGF14e*$_{ox}$ lines as compared to the WT and VC plants (Figure 5H-K, Supplementary Figure 22). On the other hand, the RWC, K^+ content, and osmolytes accumulation was significantly higher in *OsGF14e*$_{si}$ lines and lower in the *OsGF14e*$_{ox}$ lines (Figure 5J, Supplementary Figure 22). The negative role of *Os*GF14e in regulating salinity tolerance made us curious if the protein can also regulate *Os*EG45. Excitingly, the relative transcript abundance of *OsEG45* was found to be higher in *OsGF14e*$_{si}$ lines and lower in *OsGF14e*$_{ox}$ lines as compared with the WT and VC lines suggesting that the salinity tolerance of *OsGF14e*$_{si}$ plants could be mediated through an increased expression of *OsEG45* (Figure 5L-M).

The next pertinent point was to understand how *Os*GF14e modulates the expression of *OsEG45*. Since *Os*GF14e is known to possess DNA binding activity (Schultz et al., 1998), its possible interaction with the *OsEG45* promoter was analyzed using yeast one-hybrid (Y1H) assay. However, no interaction was detected between them suggesting involvement of some other regulatory mechanism (Supplementary Figure 23).

Lower *Os*GF14e abundance reduced GA accumulation and imparted salinity tolerance in rice

The germination efficiency of the few seeds that could be collected from the *ox*$_c$ and *OsGF14e*$_{si}$ lines was analyzed and compared with the WT, VC, *ox*$_n$ and *OsGF14e*$_{ox}$ lines. It was observed that none of the seeds from *ox*$_c$ and *OsGF14e*$_{si}$ lines germinated while the germination percentage for the other lines was more than 90 % (Figure 6A-D). Since GA had long been

known to regulate dwarfism, pollen sterility and seed germination, we were curious whether the abnormalities in both *ox*$_c$ and *OsGF14e*$_{si}$ lines were mediated by GA pathway. Indeed, exogenous GA_3 treatment resulted in 90-95 % seed germination in the otherwise dormant *ox*$_c$ and *OsGF14e*$_{si}$ seeds. In addition, the α-amylase activity was found to be significantly low in the *ox*$_c$ and *OsGF14e*$_{si}$ lines which were improved in response to exogenous GA_3 treatment (Figure 6B, 6D). Further, the GA_3 content was measured from *ox*$_c$, *ox*$_n$, and *OsGF14e*$_{si}$ lines and compared with WT and VC lines. Intriguingly, the GA_3 content was found to be significantly lower (undetectable) in both *ox*$_c$ and *OsGF14e*$_{si}$ lines compared with the WT and VC lines while no significant alteration in the GA_3 content of *ox*$_n$ lines was observed (Figure 6E). This observation strongly suggested that the *Os*r40g3-mediated degradation of *Os*GF14e in the *ox*$_c$ lines hindered GA metabolism leading to pollen sterility and seed dormancy.

Further, we were curious about any relationship between the reduced GA content and higher abundance of *OsEG45* transcripts in the *OsGF14e*$_{si}$ plants. To investigate this, the expression of *OsEG45* was analyzed under altered GA conditions. Excitingly, when rice seedlings were treated with paclobutrazol, an inhibitor of GA biosynthesis, the *OsEG45* gene expression was significantly up-regulated while exogenous application of GA_3 reduced its transcript accumulation (Figure 6F).

Discussion

The R40 family of lectin proteins was known to play a vital role in regulating drought and salinity stress tolerance in plants (Moons et al., 1995; Jiang et al., 2012b). Among these proteins, the putative *Os*r40c1 was found to play a fundamental role in imparting drought tolerance in rice and tobacco (Sahid et al., 2020). However, the functional aspects of the other *Os*R40 proteins remained unexplored till date. In the present investigation, it was observed that among all the *Os*R40 family members, *Osr40g3* displayed the highest expression in response to salinity stress (Supplementary Figure 3). This prompted us to explore how *Osr40g3* imparts salinity tolerance in plants. To investigate this, 8 *indica* rice cultivars were selected and analyzed for their salinity stress response. Excitingly, it was observed that the expression of *Osr40g3* positively correlated with the salinity tolerance potential with its highest expression in the tolerant Nonabokhra

cultivar and lowest expression in the sensitive MTU1010 cultivar (Supplementary Figure 1). This strongly indicated a salinity-responsive role of *Osr40g3* in rice.

To further validate this clue, *Osr40g3*-overexpressing transgenic rice lines (ox_c) were generated harboring the recombinant *35S::Osr40g3* construct. The resulting transgenic lines exhibited significantly improved salinity tolerance in comparison with the WT and VC plants (Figure 1, Supplementary Figure 4). Surprisingly, however, most of the transgenic lines failed to set seeds suggesting a negative role of *Osr40g3* in seed development (Figure 1). In consistence with this observation, the transgenic rice flowers appeared to be shorter with mostly sterile pollen grains (Supplementary Figure 7). On contrary, when the same construct was introduced into *Arabidopsis*, the transgenic lines (*ec*) ectopically expressing *Osr40g3* displayed improved salinity tolerance but no defect in seed development (Supplementary Figure 5-6). Unlike rice, the floral morphology of the transgenic *Arabidopsis* lines also exhibited no phenotypic alteration (Supplementary Figure 8).

A failure to set seeds can result from a defect in the male part, female part or both in the flower. To check these possibilities, the WT rice plants were crossed with the *Osr40g3* overexpressing transgenic lines. Crossing the emasculated WT plants with the transgenic plants as a male parent failed to produce any seed thus confirming the pollen sterility in the transgenic lines. On contrary, when the emasculated transgenic plants were pollinated with the WT pollen grains, hybrid seeds were obtained indicating no defect in the pistil of the transgenic flowers (Supplementary Figure 9). This observation strongly suggested that *Osr40g3* specifically affected the pollen viability while the pistil remained unaffected.

Since *Osr40g3* gene was overexpressed under control of a constitutive promoter, the next pertinent question was whether the gene possesses a tissue-specific expression pattern. Indeed, the gene displayed highest expression level in the leaves during most of the developmental phases with no expression in the stamen (Figure 2). Furthermore, the constitutive overexpression of *Osr40g3* in flowers and stamens diminished the expression of one of the important regulators of pollen viability, *OsAGL65* (Benjamin et al. 2009). In line with this observation, the *Osr40g3* gene was next cloned under control of the native promoter (*Osr40g3pro::Osr40g3*) and transgenic rice lines (ox_n) were generated harboring this recombinant construct. Interestingly, in

addition to salinity tolerance, all these transgenic lines showed proper seed development thus rescuing the pollen sterile phenotype (Figure 3, Supplementary Figure 12). These observations indicated that *Osr40g3* followed a precise tissue-specific expression pattern which is crucial for proper pollen viability and seed development in rice.

Identifying the interacting protein partners of *Os*r40g3 was the next relevant point in solving the mechanism of the protein in rice. Intriguingly, it was identified that *Os*r40g3 interacted with several protein partners to execute its role in salinity stress tolerance. *Os*r40g3 was identified to interact with the *Os*EG45 protein in the salinity stressed rice leaves (Figure 4). EG45 is a salinity stress-responsive expansin-like glycoprotein that showed endoglucanase-like function and helped in cell wall modification (Ludidi et al., 2002). Cell wall modification is a common phenomenon observed in the osmotically stressed cells (Gall et al., 2015). Several expansin genes were reported to be up-regulated under osmotic stress. For example, the expression of the rose expansin gene, *RhEXPA4*, was found to be induced in response to salinity stress and its ectopic expression in *Arabidopsis* led to salt-tolerant phenotype (Lü et al., 2013). Similarly, transgenic tobacco expressing the wheat expansin gene *TaEXPB23* displayed improved salinity tolerance (Han et al., 2012). In addition, up-regulation of expansin gene expression was also reported under water deficit conditions in many plants (Wu et al., 2001; Guo et al., 2011; Li et al., 2013). In the present investigation, overexpression of *OsEG45* gene led to improved salinity tolerance while silencing of this gene displayed sensitivity towards salinity stress (Figure 5). This study suggested that *Os*r40g3 significantly improved salinity stress tolerance in rice by positively regulating the *Os*EG45 protein. Since the *Os*r40g3 protein could also interact with *At*EXLB2, the *Arabidopsis* ortholog of *Os*EG45, these transgenic *Arabidopsis* lines displayed salinity stress tolerance (Supplementary Figure 16).

On the other hand, when a cDNA library from rice flowers was used, the *Os*r40g3 was found to interact with *Os*GF14e (Figure 4). The *Os*GF14e is a member of the GF14 protein family (14-3-3 proteins) and modulates several stress responses as well as plant development (Chen et al., 2006). For example, the rice GF14 family proteins like *Os*GF14b, *Os*GF14c, *Os*GF14e and *Os*GF14f were found to interact with different target proteins to critically regulate the signaling responses during biotic stress (Chen et al., 2006). Furthermore, *Os*GF14e was demonstrated to

negatively regulate sheath blight and bacterial blight resistance in rice (Manosalva et al., 2011). Also, the suppression of *Os*GF14e could produce susceptibility towards panicle blast (Manosalva et al., 2011; Liu et al., 2015, 2016). In addition, *Os*GF14e interacted with DOF ZFP transcription factors that were activated by developmental signals in plants (Cooper et al., 2003).

Earlier evidences suggested that low accumulation of GF14e protein was associated with sterile pollen grains in maize (Datta et al., 2002). Again, the silencing of *OsGF14e* gene displayed stunted growth and poor seed development in rice (Manosalva et al., 2011). A subsequent study by Liu et al. (2016) precisely demonstrated that all the *OsGF14e*-silenced lines failed to develop seeds except two lines with less *OsGF14e* silencing. Similarly, in the present study, *Os*r40g3 was found to negatively regulate the stability of *Os*GF14e protein which presumably led to impaired seed development in the ox_c transgenic lines (Figure 1, 4). Supporting this, the $OsGF14e_{si}$ lines also displayed pollen sterility and failed to produce seeds which can be corroborated with the previous reports (Figure 5). Accumulating evidences also suggested that rice GF14 family members interacted with site specific DNA binding proteins like *Em*BP1 and tissue specific transcription factor, VP1 to regulate signaling responses in a spatial manner (Schultz et al., 1998). This supported the highly precise and tissue-specific function of the GF14 proteins in plants. Consistent with these reports, out of the eight GF14 family members, the *Os*GF14e and *Os*GF14f showed higher accumulation in flowers and panicles which corroborated with our present observation (Chen et al., 2006).

Furthermore, the few seeds that developed in the transgenic rice lines (ox_c) constitutively overexpressing the *Osr40g3* gene as well as the *OsGF14e* silencing lines ($OsGF14e_{si}$) displayed complete inhibition of germination. Since, dwarfism, pollen sterility, and seed germination, are widely known to be regulated by GA, we assumed that these transgenic lines might have a defect in GA metabolism. Indeed, exogenous application of GA_3 could rescue the germination inhibition in the transgenic seeds supporting this hypothesis (Figure 6). In addition, the α-amylase activity was also found to be impaired in the transgenic seeds that were relieved by GA_3 treatment. Finally, the lower accumulation of GA content in these transgenic lines further supported the alteration in the GA metabolism (Figure 6). These observations corroborated with the previous report where the *OsGF14e*-silenced rice plants also exhibited a defect in GA

metabolism (Liu et al., 2016). However, how *Os*GF14e integrates the GA pathway with pollen development is an exciting area that needs to be explored in the future.

Although *Os*GF14e has several orthologs in *Arabidopsis*, the transgenic plants ectopically expressing *Osr40g3* (*ec* lines) displayed normal seed development. To understand this unusual observation, we checked if these orthologs in *Arabidopsis* could interact with the *Os*r40g3 protein through Y2H analysis. However, none of them could interact with *Os*r40g3 suggesting a high specificity of the *Os*r40g3-*Os*GF14e interaction (Supplementary Figure 16). It was reported that the *Arabidopsis* GF14 family can be broadly classified into two groups, the epsilon group and the non-epsilon group (Daugherty et al., 1996; Sehnke et al., 2006). The non-epsilon group included the omega, psi, mu, nu and chi proteins which showed close homology with *Os*GF14e. Among them, the *At*GF14-chi was reported to be highly expressed in the *Arabidopsis* flowers (Daugherty et al., 1996). Nevertheless, the varied C-terminal domain of the GF14 family members was reported to determine their functional variation and specificity in plants (Sehnke et al., 2006). This structural distinctiveness of *Os*GF14e from its *Arabidopsis* orthologs provided a possible answer why *Os*r40g3 ectopic expression failed to impede seed development in *Arabidopsis*. Interestingly, other members of *Os*r40 family also did not interact with *Os*GF14e suggesting the specific interaction of *Os*r40g3 with *Os*GF14e.

The *Os*r40g3 was found to interact with *Os*GF14e in the stamens only when it was overexpressed under a constitutive promoter. In the WT, however, the *Os*r40g3 is not expressed in the stamen ruling out its scope of interaction with *Os*GF14e. We, therefore, wondered why this highly specific interaction evolved and if it has any role in modulating *Os*r40g3-mediated salinity stress tolerance in rice. To explore this possibility, we analyzed the salinity tolerance potential of the $OsGF14e_{ox}$ and $OsGF14e_{si}$ lines. It was observed that the $OsGF14e_{si}$ plants displayed salinity stress tolerance while $OsGF14e_{ox}$ lines showed sensitivity to salinity stress (Figure 5). Moreover, the higher transcript abundance of *OsEG45* in the $OsGF14e_{si}$ plants and its lower abundance in the $OsGF14e_{ox}$ plants suggested an intricate signaling crosstalk between *Os*r40g3, *Os*GF14e and *Os*EG45 in regulating salinity tolerance in rice. It was further observed that the *Os*r40g3-mediated proteosomal degradation of *Os*GF14e resulted in a lower accumulation of endogenous GA in plants. A reduced GA level was again found to upregulate

OsEG45 expression thus explaining its elevated transcript abundance in the *OsGF14e*$_{si}$ lines. Therefore, it can be concluded that *Os*r40g3 negatively regulated *Os*GF14e which resulted in perturbation of GA metabolism. The reduced GA content in turn induced the expression of *OsEG45*. In addition, *Os*r40g3 positively regulated *Os*EG45 by directly interacting with it (Figure 7). Together, the present investigation unraveled a novel *Os*r40g3-*Os*GF14e-*Os*EG45 signaling module in mitigating salinity stress that may be exploited for developing salinity tolerant rice in future crop improvement programs.

Materials and methods

Plant material and stress treatment

The seeds of different *indica* rice cultivars like Nonabokra, Ranjit, Khitish, IR64, Swarna sub1, Jaldi13, MTU1010, and Vandana were procured from the Chinsurah Rice Research Station, West Bengal, India. Plants were grown in a greenhouse under the optimum condition at day/night temperature regime of 30°-35°C/22°-29°C and 60-65 % relative humidity with 12 h photoperiod. For salinity stress, seeds were surface sterilized using 4 % sodium hypochlorite followed by 0.2 % bavistin treatment, germinated and grown on filter papers wetted with water for 15 d. Hundred seedlings of each cultivar were treated with 200 mM NaCl solution for 5 d as standardized before (Kurniasih et al., 2013; Sahid et al., 2020). For salt stress treatment of soil-grown plants, the pots were irrigated with 200 mL of 200 mM NaCl solution per day, and data was recorded after 5 d of salt treatment (Amirjani, 2012). For the control set, the same volume of distilled water was used.

A. thaliana seeds of Columbia ecotype (Col-0) were procured from Nottingham Arabidopsis Stock Center (NASC), UK and were grown and maintained in a growth chamber at 22°C under 16 h light/8 h dark cycle as standardized before (Datta et al., 2015). 30 d old plants were exposed to salinity stress by irrigating with 20 mL of 200 mM NaCl solution every alternate day as standardized before (Datta et al., 2015). For the control set, the same volume of distilled water was used.

Morphological analyses

Different morphological parameters like shoot and root length, seedling dry weight, and percentage of rolled leaves were analyzed under control and stressed conditions. Tissue was dried at 50°C for 3 d to measure the dry weight. The RWC was estimated after salinity stress exposure following Ma et al. (2018).

Estimation of different biochemical compounds

Proline and glycine betaine contents were measured by spectrophotometric method from tissue samples collected from control and treated plants according to Grieve and Grattan (1983) and Woodrow *et al.* (2016) respectively. The chlorophyll content was measured according to Lichtenthaler (1987). The H_2O_2 content was measured following Yin et al. (2010).

RNA Extraction and qRT PCR Analysis

Total RNA was extracted using the Trizol method from tissues of rice and *Arabidopsis* plants. Complementary DNA (cDNA) was synthesized using iScript™ cDNA Synthesis Kit (Bio-Rad) following the manufacture's protocol. The qRT PCR analysis was performed in the CFX96 Touch™ Real-Time PCR Detection System (Bio-Rad) using iTaq Universal SYBR Green Supermix (Bio-rad) and gene-specific primers (Table S1). The gene expression was normalized based on the relative quantification method. The *Actin* gene of rice and *Arabidopsis* was used as a reference gene. Three technical replicates and three biological replicates were considered for each analysis.

Vector Construction and Plant Transformation

For development of overexpression lines, the full-length gene of *Osr40g3* (LOC112936024) was amplified by PCR using gene specific primers (Table S1). The amplified product was inserted into pGEM®-T Easy Vector Systems (Promega) and subsequently sub-cloned between the *EcoRI* and *BamHI* restriction enzyme (RE) sites of *pEGAD* vector under the control of a constitutive *CaMV35S* promoter. The recombinant construct (*35S::Osr40g3*) was transformed into the background of *indica* rice cultivar khitish (IET4095) following *Agrobacterium*-mediated genetic transformation method (Datta et al., 2000; Sahid et al., 2020). The putative transformants were screened for herbicide resistance, and positive lines were confirmed by genomic DNA PCR

using *bar* gene-specific primers. Positive lines, along with WT and VC plants, were grown in a greenhouse with optimum condition as described before. The same construct was used to transform *Arabidopsis* plants of Col-0 ecotype via *Agrobacterium*-mediated floral-dip method as standardized before (Clough and Bent, 1998; Datta et al., 2015). The independent transgenic lines generated were maintained and grown up to T_2 generations in a growth chamber as described above.

To clone the promoter region of *Osr40g3* gene, the 1,315 bp upstream sequences from +1 site of *OsR40g3* gene was selected. The fragment was amplified from rice genomic DNA by PCR using sequence specific primers. The amplified native promoter was inserted between the *AgeI* and *PacI* RE sites of the recombinant vector *35S*::O*sr40g3* to generate the construct, *Osr40g3pro*::*Osr40g3*. The promoter fragment was also sub-cloned between the *BamHI* and *BglII* RE sites of *pCAMBIA1304* vector to generate the *Osr40g3pro*::*GUS* construct. The constructs were used for *Agrobacterium*-mediated genetic transformation of rice as described above. The independent transgenic lines generated were maintained and grown up to T_2 generations under greenhouse conditions as described above.

For generation of the overexpression constructs for *OsEG45* and *OsGF14e* genes, the full length sequences were amplified by PCR using gene specific primers. The amplified products were cloned into pGEM®-T Easy Vector Systems (Promega) followed by sub-cloning between the *EcoRI* and *BamHI* RE sites of *pEGAD* vector and the *SpeI* and *BamHI* sites of *pVYNE* vector respectively. For generation of silencing constructs for *OsEG45* and *OsGF14e* genes, the 266 bp and 335 bp coding sequences, respectively, were amplified by PCR using the gene specific primers and cloned into pRNAi-GG vector by Golden Gate cloning method following Yan et al. (2012). The constructs were used for *Agrobacterium*-mediated genetic transformation of rice as described above.

Morphological Analysis of Transgenic Plants

Several morphological parameters like plant height, number of tillers, shoot and root dry weights, panicle length, number of panicles/plant, number of flowers/panicle, number of grains/panicle, and floral morphology were analyzed from the WT, VC, and transgenic rice plants. In case of *Arabidopsis*, plant height, rossette diameter, floral morphology, silique length,

number of silique/plant, number seeds/silique, and seed yield/plant were measured from WT, VC and transgenic lines. Floral morphology of both rice and *Arabidopsis* plants were studied and documented under zoom stereo trinocular microscope (Magnus MSZ-RR LED). For salt stress assay, different morphological parameters were analyzed under control and stressed conditions as described above.

Estimation of Na^+ and K^+ contents

The Na^+ and K^+ content were measured by flame photometer (Systronics, model:128) following Nublat et al (2001) with slight modifications. Briefly, leaves collected from control and stressed plants and dried at 80° C for 24 hr. The dried samples were then incubated in 0.1 M nitric acid for 30 minutes. The extract was filtered and analyzed.

Estimation of lipid peroxidation and ion leakage percentage

The lipid peroxidation of shoots from control and stressed plants was analyzed through measuring MDA content following Yin et al. (2020). Briefly, 0.2 g shoot tissue was homogenized in 10% tricholoroacetic acid (w/v) and supernatant was mixed with 0.67% (w/v) thiobarbitiuric acid. The mixture was heated and cooled. After centrifugation, the supernatant was collected and absorbance (A) was measured at 450, 532 and 600 nm.

The leaves from control and stressed plants were used to determine the relative electrolyte leakage by analyzing their relative conductivity in solution following Cao et al. (2007). The conductivity was measured using a conductivity meter (Systronics).

Pollen viability assay

For I_2-KI staining, mature pollen grains of rice were stained with 2 % I_2-KI (w/v) solution and observed under bright field microscope (Leica DM IL LED S-80) according to Chuun et al. (2007). For FDA staining, a pollen viability solution (PVS) was prepared with 0.001 % (w/v) fluorescein diacetate, 290 mM sucrose, 1 mM KNO_3, 0.16 mM boric acid, and 1.27 mM $Ca(NO_3)_2$. The mature pollen grains of rice and *Arabidopsis* were incubated in PVS at dark for 15 min at 28°C and centrifuged. The pellet was resuspended in PVS without FDA and observed under fluorescence microscope (Leica DM IL LED S-80) using 488 nm excitation and 510 nm

emission wavelengths (Muhlemann et al. 2018). For *Arabidopsis* pollen grains, Alexander staining was performed according to Schofta et al. (2011) and examined under bright field microscope (Leica DM IL LED S-80). At least 500 pollen grains were considered for each sample.

In vitro pollen germination assay

The *in vitro* pollen germination assay was performed according to Li et al. (2018). Briefly, the mature pollen grains collected from rice flowers were spread onto pollen germination medium, pH 6.0, containing of 15 % (w/v) sucrose, 0.01 % (w/v) boric acid, 1 mM $Ca(NO_3)_2$, and 0.3 % (w/v) low melting agarose and were incubated at 25°C under humid condition. After 4 h of incubation, pollen germination was analyzed and documented under bright field microscope (Leica DM IL LED S-80).

For *in vitro* pollen germination of *Arabidopsis* a solid pollen germination medium was used. The mature pollen grains were collected and spread on the pollen germination medium containing 0.01 % H_3BO_4 (w/v), 5 mM $CaCl_2$, 5 mM KCl, 1 mM $MgSO_4$, 10 % sucrose (w/v), and 0.1 % agarose (Boavida and McCormick, 2007). The pollen germination was examined under bright field microscope (Leica DM IL LED S-80) after 6 h incubation.

Hybridization of rice plants

The flowers of WT plants were emasculated and considered as female parent whereas the transgenic rice plants (ox_c) harboring the *35S::Osr40g3* construct were considered as male parent. In another set, the transgenic rice plants (ox_c) harboring the *35S::Osr40g3* construct were emasculated and considered as female parent and hybridized with WT as male parent. Hybridization was carried out as standardized before (Paul et al. 2014). In both cases the number of hybrid seeds was measured.

Histochemical GUS assay

Samples from different tissues under various developmental stages were collected from the transgenic rice lines harboring the *Osr40g3pro::GUS* construct. Samples were stained with GUS staining solution (50 mM sodium phosphate, pH 7.0, 10 mM EDTA, 0.5 mM $K_3[Fe(CN)_6]$, 0.5 mM $K_4[Fe(CN)_6]$, 0.1 % (v/v) Triton X-100, and 1 mM X-glucuronide) following Jefferson et

al.1987. The stained samples were visualized under zoom stereo trinocular microscope (Magnus MSZ-RR LED).

Y2H Analysis

Y2H analysis was performed to identify the protein partners of *Osr40g3* protein using the Matchmaker® Gold Yeast Two-Hybrid System (Takara) following the manufacturer's protocol. The *Osr40g3* gene was inserted into the *EcoRI* and *BamHI* RE sites of the bait vector, *pGBKT7* (Takara). The recombinant *BD-Osr40g3* bait construct was transformed into yeast following manufacturer's protocol. The other members of *Os*R40 family like *Os*r40c1, *Os*r40g2, *Os*r40c2 and putative *Os*r40c1 were also cloned into the bait vector pGBKT7 and used as recombinant bait constructs. The cDNA library was prepared from rice flowers and ligated to *pGADT7-Rec* vector using Make Your Own "Mate and Plate" Library System (Takara). To identify the interacting protein partners responsive for salinity stress tolerance, a second cDNA library was prepared from rice leaves under salinity stress condition. The recombinant plasmids were co-transformed into yeast Y2H Gold strain (Takara). The transformed yeast strains were grown on DDO (SD/-Leu/-Trp) and QDO/X/A (SD/–Ade/–His/–Leu/–Trp/X-α-Gal/Aureobasidin-A) media. Positive clones were selected and analyzed by sequencing following the manufacturer's instructions to identify the interacting protein partners. To analyze the interaction of *Os*r40g3 with the orthologs of *Os*EG45 and *Os*GF14e in *Arabidopsis*, the *At*EXLB2 and 12 *At*GF14 proteins were cloned into the *pGADT7-Rec* vector and used as prey for the *BD-Osr40g3* bait. Y2H analysis was performed as describes above. The *BD-p53* and *AD-T-antigen* interaction was used as a positive control. The empty *BD* and *AD-T-antigen* interaction was used as a negative control.

BiFC assay

For BiFC assay, the *Osr40g3* gene without stop codon was inserted into the vector *pVYCE* between *ApaI* and *BamHI* RE sites to obtain *35S::Osr40g3-cVenus* construct. The *OsGF14e* and *OsEG45* genes were cloned into *SpeI* and *BamHI* RE sites and *EcoRI* and *BamHI* RE sites of *pVYNE* vector to generate the *35S::OsGF14e-nVenus* and *35S::OsEG45-nVenus* constructs respectively (Waadt et al. 2008). The recombinant constructs were transformed into *Agrobacterium tumifaciens* strain GV3101. Then, the *Agrobacterium* strain was used to infiltrate

onion epidermal cells (Yang et al., 2014). The fluorescence signal for Venus protein was detected at the excitation wavelength of 514 nm using a confocal laser scanning microscope (Olympus FluoView™ FV1000). The *35S::Osr40g3-cVenus* construct with empty *35S::nVenus* vector was considered as negative control.

Co-IP and immunoblot analysis

The rice embryo calli transformed with *35S::Osr40g3-HA* and/or *35S::OsGF14e-cMyc* were used for total protein isolation (Chen et al. 2019). The samples were extracted in lysis buffer (20 mM Tris□Cl pH 7.5, 150 mM NaCl, 0.5 % Triton□X□100 (v/v) and protease inhibitor, Thermo Scientific) at 4°C and centrifuged at 13,000 rpm for 30 min at 4°C. Supernatants were collected and mixed with 20 µL anti-HA-agarose beads and incubated overnight following the manufacturer's instructions (Pierce™ HA-Tag IP/Co-IP Kit, Thermo Fisher Scientific). The HA-tagged protein was eluted and quantified by Bradford method (Bradford, 1976). Equal amount of protein was used for immunoblot analysis using anti-HA antibody (1:1000 dilution, Sigma) and anti-cMYC antibody (1:1000 dilution, Agrisera). Immunoblot against anti-α-Tubulin antibody (1:1000 dilution, Agrisera) was used as loading control. The co-immunoprecipitation assay for *Os*r40g3-HA and *Os*EG45-cMyc interaction was similarly performed. For proteasomal degradation inhibitor assay, the transformed rice calli were incubated in dark for 10 d at 37°C. The calli were then incubated with 10 µM MG132. After 4 h of incubation, proteins were isolated from the calli and used for immune blot analysis as described above (Garcia-Cano et al. 2014).

Multiple sequence alignment analysis

The protein sequences of *Arabidopsis* GF14 family members and *Os*GF14e were retrieved from NCBI database. The sequences were subjected for multiple sequence alignment using PRALINE multiple sequence alignment tool (Simossis and Heringa, 2005).

Y1H analysis

To identify the interaction of *OsGF14e* protein with *OsEG45* promoter, the 1707 bp upstream sequence from +1 site of *OsEG45* gene was amplified using PCR and cloned into the *KpnI* and

SacI RE sites of the *pAbAi* vector (Takara). On the other hand, the *OsGF14e* gene was amplified by PCR and cloned into pGADT7-Rec vector (Takara) following manufacturer's protocol. The recombinant constructs was transformed into Y1H gold strain and yeast one hybrid assay was performed using Matchmaker® Gold Yeast One-hybrid screening system (Takara) following the manufacturer's protocol. The transformed yeast strains were grown on SD/-Leu and SD/–Leu/Aureobasidin-A media.

Seed germination and α-amylase assay

The seeds collected from WT, VC, transgenic lines (ox_c, ox_n, $OsGF14e_{ox}$, *and* $OsGF14e_{si}$) were surface sterilized with 4 % sodium hypochlorite solution followed by 0.2 % bavistin treatment and placed on MS medium with and without GA_3 (5 µM/mL) for germination under dark for 7 d. Estimation of α-amylase activity was carried out following Shen et al. (2019).

Estimation of endogenous GA

The GA_3 content was measured using high performance liquid chromatography following Liu et al. (2021). Briefly, the leaves were homogenized and extracted with pre chilled 80% methanol for 20h at 4°C. After centrifugation, the supernatant was dried using vacuum concentrator. The samples were dissolved 100 in µl ultrapure methanol supplemented with 0.1 M glacial acetic acid. After filtration, the sample was analyzed using Waters HPLC system multi-dimensional liquid chromatography (model 2695) with C18 analytical column. The flow rate was 1 ml min^{-1} and column temperature was set at 30°C. The chromatogram was analyzed by Empower 3.0 software.

Exogenous GA and paclobutrazole treatment

The 15 d old seedlings were treated with 5 µM GA_3 and 2 µM paclobutrazol solutions for 48 h (Yang et al., 2004; Schmidt et al., 2014). Total RNA was extracted from seedlings and the expression of *OsEG45* gene was analyzed through qRT-PCR.

Statistical analysis

Statistical analysis was performed using GraphPad Prism version 8.3.0 software (GraphPad Software, San Diego, California USA). The variation of morphological, and biochemical

parameters as well as the relative transcript abundance among genotypes and treatments were analyzed following two-way ANOVA followed by Sidak's multiple comparison tests. To compare the morphological parameters between WT, VC and transgenic lines, one-way ANOVA followed by Dunnett's multiple comparison tests were performed. To identify the difference between two sets of data, the statistical significance at $P \leq 0.05$ was considered. Details of replicates, sample size, and the significance levels of P-values were indicated in respective figure legends. The data were represented as mean ± standard error of mean (SEM).

Acknowledgement

This work has been supported by the Department of Science and Technology and Biotechnology, Government of West Bengal, India [BT(Budget)/RD-29/2016] and University Grant Commission, Government of India, India [UGC-CAS (Phase VII)]. We thank the central instrumentation facility of the Department of Botany, University of Calcutta and Department of Botany, Dr. A. P. J. Abdul Kalam Government College as well as the confocal microscopic facility of DBT-IPLS, Department of Biochemistry, University of Calcutta. We thank Prof. Jörg Kudla (University of Munster, Germany) for providing the *pVYNE* and *pVYCE* vectors and Prof. Prabod Trivedi (CSIR-National Botanical Research Institute, India) for kindly sharing the *Agrobacterium tumefaciens* GV3101 strain.

Author contributions

RD and SP conceived and designed the original research plan; CR and SS performed the experiments; RD and SP analyzed the data; RD and SP wrote the manuscript with contributions from CR and SS.

Figure Legends

Figure 1. Transgenic rice lines constitutively overexpressing *Osr40g3* (*ox$_c$*) displayed improved salinity tolerance but impaired seed development. Different morphological parameters of the transgenic lines harboring the *35S::Osr40g3* construct (*ox$_c$* lines) along with WT and VC (*35S::GFP*) plants were analyzed. The transgenic lines exhibited shorter plant height with impaired seed development. The WT, VC and transgenic *ox$_c$* lines were exposed to salinity stress for 5 d and analyzed. The transgenic lines indicated improved salinity stress tolerance over WT and VC lines. (A) WT, VC and 3 representative independent *ox$_c$* lines at reproductive stage, (B) overexpression construct, (C) panicles, (D) grain morphology (empty grains in transgenic lines), (E) plant height, (F) number of tillers, (G) numbers of panicles/plant, (H) shoot dry weight, (I) root dry weight, (J) panicle length, (K) numbers of flowers/panicle, (L) number of grains/panicle, (M) morphological response of WT, VC and 3 representative independent *ox$_c$* lines under salinity stress, (N) Total chlorophyll content, (O) rolled leaf percentage, (P) relative water content, (Q) relative ion leakage percentage, and (R) relative transcript abundance of *Osr40g3* gene in response to salinity stress. Ten independent transgenic lines (T_0) were considered for morphological analysis. The stress assay was independently repeated thrice with 3 independent *ox$_c$* lines (T_0) in each set. Results were represented as mean ± SEM and the statistical difference between WT, VC and transgenic lines was denoted by 'd' at P<0.0001. n.d.: not detected.

Figure 2. ***Osr40g3* follows a precise tissue-specific expression pattern in rice.** (A) Relative transcript abundance of *Osr40g3* gene in different tissues of WT rice plants was analyzed. Highest transcript abundance was observed in the leaves while no expression was detected in the stamen. The experiment was independently repeated thrice and results were represented as mean ± SEM. Statistical difference between different samples was denoted by different letters at P<0.05 (a), P<0.01 (b), and P<0.0001 (d). (B) The *Osr40g3pro::GUS* construct. (C) Representative image of histochemical GUS staining showing *Osr40g3* promoter activity in different tissues under various developmental stages. The experiment was independently repeated thrice. n.d.: not detected.

Figure 3. O**verexpression of *Osr40g3* under control its native promoter (*ox$_n$* lines) improved salinity tolerance and with proper seed development**. Different morphological parameters of 3 independent transgenic lines (*ox$_n$*) harboring the *Osr40g3pro::Osr40g3* construct were recorded and compared with WT and VC (*35S::GFP*) plants. No phenotypic abnormality was observed. The WT, VC and 3 independent transgenic *ox$_n$* lines were exposed to salinity stress for 5 d and analyzed. The transgenic lines displayed significantly improved salinity stress tolerance over WT and VC lines. (A) Overexpression construct, (B) WT, VC and transgenic *ox$_n$* lines at reproductive stage with panicles in the inset, (C) grain morphology, (D) plant height, (E) number of tillers, (F) shoot dry weight, (G) root dry weight, (H) numbers of panicles/plant, (I) panicle length, (J) numbers of flowers/panicle, (K) number of grains/panicle, (L) morphological response of WT, VC and 3 independent *ox$_n$* lines under salinity stress, (M) total chlorophyll content, (N) rolled leaf percentage, (O) relative water content, (P) relative ion leakage percentage, and (Q) relative transcript abundance of *Osr40g3* gene in response to salinity stress. For morphological analysis, 10 biological replicates were considered for each line (T_1). The stress assay was independently repeated thrice with 3 biological replicates (T_1 lines) in each set. Results were represented as mean ± SEM and the statistical difference between WT, VC and transgenic lines was denoted by 'd' at P<0.0001. n.d.: not detected.

Figure 4. Identification of interacting protein partners of *Os*r40g3. (A) Yeast two-hybrid assay identified the interaction of *Os*r40g3 with *Os*EG45-like domain containing protein, a peroxisomal membrane protein, *Os*PMP22 and 60S ribosomal protein L35 when a cDNA library from rice leaves under salinity stress was used. The interaction of p53 protein with T-antigen was used as a positive control. The interaction of the empty BD with T-antigen was used as a negative control. (B) Relative transcript abundance of the identified partners in response to salt stress. *OsEG45* was found to be salt-responsive. Results were represented as mean ± SEM and the statistical difference between control and salt conditions was denoted by 'd' at P<0.0001. (C) When a cDNA library from rice flowers was used, yeast two-hybrid analysis identified the interaction of *Os*r40g3 with *Os*GF14e, *Os*AGL20 and *Os*AP2-like proteins. The interaction of p53 protein with T-antigen was used as a positive control. The interaction of the empty BD with T-antigen was used as a negative control. (D) BiFC analysis confirmed the interaction of *Os*r40g3 protein with *Os*EG45 and *Os*GF14e. Venus fluorescence, bright field, and merged

images were represented for each set of constructs. (E) Co-immunoprecipitation analysis was performed for the interaction of *Os*r40g3-HA with *Os*EG45-cMyc followed by immunoblot analysis using anti-HA and anti-cMyc antibody. The experiment was independently repeated thrice. (F) Interaction of *Os*GF14e-cMyc with *Os*r40g3-HA was similarly confirmed through co-immunoiprecipitation assay followed by immunoblot analysis using anti-HA and anti-cMyc antibody. The experiment was independently repeated thrice. (G) Proteasomal degradation assay of *Os*GF14e-cMyc was performed using a proteasomal inhibitor, MG132 followed by immunoblot analysis using anti-cMyc and anti-HA antibody. The amount of *Os*GF14e-cMyc was reduced to a significant level when co-expressed with *Os*r40g3-HA. The experiment was independently repeated thrice. Immunoblot analysis using anti-α tubulin antibody against total protein was used as loading control.

Figure 5. *Os*EG45 plays a positive role in regulating salinity tolerance while *Os*GF14e plays a negative role. The WT, VC (*35S::GFP*) and 3 independent transgenic lines for each of the *OsEG45* overexpressing ($OsEG45_{ox}$) and silencing ($OsEG45_{si}$) lines were exposed to salinity stress for 5 d and analyzed. The $OsEG45_{ox}$ lines exhibited significantly improved salinity stress tolerance over WT and VC lines while the $OsEG45_{si}$ displayed sensitivity. (A) Morphological response of WT, VC and 3 independent $OsEG45_{ox}$ and $OsEG45_{si}$ lines under salinity stress, (B) total chlorophyll content, (C) rolled leaf percentage, (D) relative water content, (E) relative ion leakage percentage, and (F) relative transcript abundance of *Osr40g3* gene in response to salinity stress. The stress assay was independently repeated thrice with 3 biological replicates in each set with T_1 plants. The WT, VC and independent transgenic lines for each of the *OsGF14e* overexpressing ($OsGF14_{ox}$) and silencing ($OsGF14_{si}$) lines were exposed to salinity stress for 5 d and analyzed. The $OsGF14_{ox}$ lines exhibited severe sensitivity to salinity stress while the $OsGF14e_{si}$ displayed improved salinity tolerance over the WT and VC plants. (G) Morphological response of WT, VC and representative 3 independent $OsGF14e_{ox}$ and $OsGF14e_{si}$ lines under salinity stress, (H) total chlorophyll content, (I) rolled leaf percentage, (J) relative water content, (K) relative ion leakage percentage, and (L) relative transcript abundance of *Osr40g3* gene in response to salinity stress. The stress assay was independently repeated twice with 5 independent $OsGF14_{ox}$ and $OsGF14_{si}$ lines (T_0). (M) The relative transcript abundance of *OsEG45* gene was analyzed in 3 independent $OsGF14_{ox}$ and $OsGF14_{si}$ lines. The expression was found to be

significantly down-regulated in the *OsGF14*$_{ox}$ lines and up-regulated in the *OsGF14*$_{si}$ lines. Results were represented as mean ± SEM and the statistical difference between WT, VC and transgenic lines was denoted by different letters at P<0.05 (a), P<0.01 (b), P<0.001 (c), and P<0.0001 (d). n.d.: not detected.

Figure 6. Constitutive overexpression of *Osr40g3* and silencing of *OsGF14e* interfered with GA metabolism in rice (A) Seed germination assay for WT, VC (*35S::GUS*) and transgenic rice lines harboring *35S::Osr40g3* (*ox*$_c$) and *Osr40g3pro::Osr40g3* (*ox*$_n$) constructs under control and GA_3 treated conditions. The experiment was independently repeated twice with 10 seeds of different independent lines. (B) Seed germination percentage and α-amylase assay for the same. Exogenous GA_3 treatment significantly improved seed germination percentage as well as α-amylase activity in the otherwise dormant *ox*$_c$ lines. The α-amylase assay was repeated thrice. (C) Seed germination assay for WT, VC, *OsGF14e*$_{ox}$ and *OsGF14e*$_{si}$ under control and GA_3 treated conditions. GA_3 treatment enabled germination of the dormant *OsGF14e*$_{si}$ seeds. The experiment was performed once since very few seeds were produced in the *OsGF14e*$_{si}$ lines. (D) Seed germination percentage and α-amylase assay for the same. Exogenous GA_3 treatment significantly improved seed germination percentage as well as α-amylase activity in the otherwise dormant *OsGF14e*$_{si}$ lines. The α-amylase assay was repeated twice. (E) The GA_3 content was analyzed from WT, VC, *ox*$_c$, *ox*$_n$, and *OsGF14e*$_{si}$ lines. GA_3 level was undetectable in the *ox*$_c$ and *OsGF14e*$_{si}$ lines. The experiment was independently repeated thrice. (F) 15 d old WT seedlings were treated with exogenous GA3 and an inhibitor of GA biosynthesis, paclobutrazol (pac.) for 48 h and the relative transcript abundance of *OsEG45* was analyzed. The expression was found to be significantly down-regulated in response to GA_3 treatment while up-regulated by paclobutrazol treatment. The treatment was independently repeated thrice and analyzed. The results were represented as mean ± SEM. Statistical difference of the samples was denoted by different letters at P<0.05 (a), and P<0.0001 (d). n.d.: not detected.

Figure 7. *Os*r40g3-*Os*GF14e-*Os*EG45 module in regulating salinity tolerance in rice. Salinity stress induces the expression of *Osr40g3*. The *Os*r40g3 protein next interacts with and positively regulates *Os*EG45 protein. *Os*r40g3 also interacts with *Os*GF14e leading to its proteosomal degradation. The diminished *Os*GF14e protein accumulation reduces gibberellic

acid accumulation which further induces the expression of *OsEG45* leading to salinity tolerance in rice.

Supplementary Files

Table S1: Concentration of sodium, potassium and chloride ions in soil before and after salt treatment.

Table S2: Primers used in this study

Supplementary Figure 1. **Salinity stress assay of 8 *indica* rice cultivars**. 15 d old seedlings were treated with 200 mM NaCl solution for 5 d and morphological changes were analyzed. (A) Morphology of 8 *indica* rice cultivars in response to salinity stress. (B) After salt treatment, samples were used for qRT-PCR analysis to study the relative transcript abundance for *OsRAB16* and *Osr40g3* genes. The experiment was independently repeated thrice and results were represented as mean ± SEM. Statistical difference between samples under control and salinity stress was denoted by different letters at P<0.05 (a), P<0.01 (b), P<0.001 (c) and P<0.0001 (d).

Supplementary Figure 2. Morphological and biochemical analyses of the 8 *indica* rice cultivars in response to salinity stress. (A) Scoring of salinity stress response according of IRRI (2013), (B) seedling dry weight, (C) shoot length, (D) root length, (E) chlorophyll content, (F) proline content, (G) H_2O_2 content, and (H) glycine betaine content. Three biological replicates were considered for each experiment and results were represented as mean ± SEM. Statistical difference between samples under control and salinity stress was denoted by different letters at P<0.05 (a), P<0.01 (b), P<0.001 (c) and P<0.0001 (d).

Supplementary Figure 3. Relative transcript abundance of 5 different *Os*R40 family genes from rice shoots in response to salinity stress condition. *Osr40g3* displayed highest induction in response to salinity stress. The experiment was independently repeated thrice and results were represented as mean ± SEM. Statistical difference under control and salinity stress was denoted by different letters at P<0.05 (a), and P<0.0001 (d). n.d.: not detected.

Supplementary Figure 4. Biochemical analyses of the transgenic rice lines constitutively overexpressing the *Osr40g3* gene (ox_c lines) in response to salinity stress. (A) Proline content, (B) glycine betaine content, (C) H_2O_2 content, (D) MDA content, (E) sodium (Na^+) content, and (F) potassium (K^+) content. The experiment was performed with 3 independent transgenic lines

and results were represented as mean ± SEM. Statistical difference between the WT, VC, and ox_c lines was denoted by different letters at P<0.01 (b), P<0.001 (c) and P<0.0001 (d).

Supplementary Figure 5. **Morphological characterization of transgenic *Arabidopsis* lines ectopically expressing *Osr40g3***. Different morphological parameters of 3 independent transgenic lines harboring the *35S::Osr40g3* construct (*ec* lines) were recorded and compared with WT and VC (*35S::GFP*) plants. The transgenic lines exhibited no phenotypic abnormalities. (A) WT, VC and *ec* lines at reproductive stage, (B) siliques, (C) rosette diameter, (D) plant height, (E) silique length, (F) number of siliques per plant, (G) number of seeds per silique, and (H) seed yield per plant. Five biological replicates were considered for each line (T_2) and results were represented as mean ± SEM. No statistically significant difference was observed between WT, VC and *ec* lines.

Supplementary Figure 6. Response of transgenic *Arabidopsis* lines ectopically expressing *Osr40g3* gene under salinity stress condition. The WT, VC (*35S::GFP*) and 3 independent transgenic lines harboring the *35S::Osr40g3* construct (*ec* lines) were exposed under salinity stress for 5 d and analyzed. The transgenic lines exhibited improved salinity stress tolerance over WT and VC lines. (A) Morphological response under salinity stress, (B) relative transcript abundance of *Osr40g3* gene in response to salinity, (C) relative water content, (D) sodium (Na^+) content, (E) chlorophyll content, (F) proline content, (G) H_2O_2 content, and (H) glycine betaine content. The experiment was independently repeated thrice with T_2 plants and results were represented as mean ± SEM. Statistical difference between the samples under control and salinity stress was denoted by different letters at P<0.05 (a), P<0.01 (b), P<0.001 (c) and P<0.0001 (d). n.d.: not detected.

Supplementary Figure 7. **Floral morphology of transgenic rice lines constitutively overexpressing *Osr40g3*gene.** The floral morphology and pollen viability of 3 representative independent transgenic lines harboring the *35S::Osr40g3* construct (ox_c lines) along with the WT and VC (*35S::GFP*) plants were analyzed. The transgenic flowers appeared to be shorter than the WT and VC flowers with markedly reduced pollen viability and germination. (A) Entire flower, (B) dissected flower, (C) stamens with pistil, (D) pollen viability by I_2-KI staining method, (E) pollen viability by FDA staining method, and (F) *in vitro* pollen germination assay. For floral

morphology, 3 flowers from each of 10 independent T_0 transgenic lines were considered. For pollen viability and *in vitro* germination assay, at least 500 pollen grains from each line were studied.

Supplementary Figure 8. **Floral morphology of transgenic *Arabidopsis* lines ectopically expressing *Osr40g3*.** The floral morphology of 3 independent transgenic lines harboring the *35S::Osr40g3* construct (*ec* lines) were recorded and compared with WT and VC (*35S::GFP*) plants. No morphological alteration was observed between the transgenic, VC and WT flowers. (A) Entire flower, (B) dissected flower, (C) stamens with pistil, (D) pollen viability assay by alexander staining method, (E) pollen viability assay by FDA staining method, and (F) *in vitro* pollen germination assay. Five biological replicates were considered for each line (T_2). For pollen viability and *in vitro* germination assay, at least 500 pollen grains from each line were studied.

Supplementary Figure 9. **Crossing of WT plants with transgenic rice constitutively overexpressing *Osr40g3***. (A) Crossing of emasculated transgenic ox_c plants with WT pollen grains produced hybrid seeds while (B) crossing the emasculated WT plants with the pollens from transgenic ox_c plants failed to produce seeds. The experiment was independently repeated in three sets. Arrows indicate hybrid seeds.

Supplementary Figure 10. Relative transcript abundance of *Osr40g3* and *OsAGL65* genes in the WT and transgenic rice lines harboring the *35S::Osr40g3* construct (ox_c) from leaf, flower and stamen tissues. The experiment was independently repeated thrice and results were represented as mean ± SEM. Statistical difference between WT and ox_c lines was denoted by different letters at $P<0.05$ (a), and $P<0.001$ (c). n.d.: not detected.

Supplementary Figure 11. **Histochemical GUS assay for *Osr40g3* promoter activity in response to salinity stress**. The VC line harboring the *35S::GUS* construct was used as a control. The experiment was independently repeated thrice.

Supplementary Figure 12. **Pollen viability of transgenic rice lines overexpressing *Osr40g3* under control of native promoter.** The pollen viability of 3 independent transgenic lines harboring the *Osr40g3pro::Osr40g3* construct (ox_n lines) along with the WT and VC

(*35S::GFP*) plants were analyzed. No significant difference was observed in the pollen viability and germination efficiency of the transgenic pollen grains as compared with the WT and VC lines. (A) Pollen viability by I_2-KI staining method, (B) pollen viability by FDA staining method, and (C) *in vitro* pollen germination assay. At least 500 pollen grains from each line (T_1) were studied.

Supplementary Figure 13. Relative transcript abundance of *Osr40g3* and *OsAGL65* genes in transgenic rice line (*ox*$_n$) harboring the *Osr40g3pro::Osr40g3*construct from leaf, flower and stamen tissues. The experiment was independently repeated thrice and results were represented as mean ± SEM. Statistical difference between WT and *ox*$_n$ lines was denoted by different letters at P<0.001 (c), and P<0.0001 (d). n.d.: not detected.

Supplementary Figure 14. Biochemical analyses of the transgenic rice lines overexpressing the *Osr40g3* gene (*ox*$_n$ lines) under control of the native promoter in response to salinity stress. (A) Proline content, (B) glycine betaine content, (C) H_2O_2 content, (D) MDA content, (E) sodium (Na^+) content, and (F) potassium (K^+) content. The experiment was independently repeated thrice with 3 independent transgenic lines (T_1) and results were represented as mean ± SEM. Statistical difference between the WT, VC, and transgenic lines was denoted by different letters at P<0.01 (b), P<0.001 (c) and P<0.0001 (d).

Supplementary Figure 15. Relative transcript abundance of *OsGF14e* in leaf, root, flower and stamen of WT plant. The experiment was independently repeated thrice and results were represented as mean ± SEM. Statistical difference of the samples was denoted at P<0.0001 (d).

Supplementary Figure 16. Yeast two-hybrid assay for the interaction of *Os*r40g3 with the *Arabidopsis* orthologs of *Os*GF14e and *Os*EG45 proteins. *Os*r40g3 interacted with *At*EXLB2, the orthologs of *Os*Eg45, while no interaction between *Os*r40g3 and the orthologs of *Os*GF14e was observed. The interaction of p53 protein with T-antigen was used as a positive control. The interaction of the empty BD with T-antigen was used as a negative control.

Supplementary Figure 17. Multiple sequence alignment of *Os*GF14e protein with *Arabidopsis* GF14 family members showing structural variability at the C-terminal end.

Supplementary Figure 18. Yeast two-hybrid assay for the interaction of *Os*GF14e with all the *Os*r40 family proteins. Positive interaction was observed only in case of *Os*r40g3. The interaction of p53 protein with T-antigen was used as a positive control.

Supplementary Figure 19. Biochemical analyses of the *OsEG45* overexpressing (*OsEG45ox* lines) and silencing (*OsEG45si* lines) transgenic rice lines in response to salinity stress. (A) Proline content, (B) glycine betaine content, (C) H_2O_2 content, (D) MDA content, (E) sodium (Na^+) content, and (F) potassium (K^+) content. The experiment was independently repeated thrice with three independent transgenic lines (T_1) and results were represented as mean ± SEM. Statistical difference between the WT, VC, and transgenic lines was denoted by different letters at P<0.01 (b), P<0.001 (c) and P<0.0001 (d).

Supplementary Figure 20. **Morphological characterization of the *OsGF14e* overexpressing (*OsGF14e$_{ox}$* lines) and silencing (*OsGF14e$_{si}$* lines) transgenic rice lines**. Different morphological parameters of 5 independent *OsGF14e* overexpressing (*OsGF14e$_{ox}$* lines) and silencing (*OsGF14e$_{si}$* lines) transgenic rice lines were recorded and compared with WT and VC (*35S::GFP*) plants. The *OsGF14e$_{ox}$* lines exhibited no phenotypic abnormalities while the *OsGF14e$_{si}$* lines failed to set seeds. (A) WT, VC, *OsGF14e$_{ox}$* and *OsGF14e$_{si}$* lines at reproductive stage, (B) panicles, (C) seed morphology, (D) plant height, (E) number of tillers, (F) root dry weight, (G) shoot dry weight, (H) number of panicles per plant, (I) panicle length, (J) number of flowers per panicles, and (H) number of seeds per panicle. Five independent transgenic lines (T_0) were considered for each case and results were represented as mean ± SEM. Statistical difference between the WT, VC and transgenic lines was denoted by P<0.0001 (d).

Supplementary Figure 21. **Pollen viability of the *OsGF14e* overexpressing (*OsGF14e$_{ox}$* lines) and silencing (*OsGF14e$_{si}$* lines) transgenic rice lines.** The pollen viability of 3 independent *OsGF14e* overexpressing (*OsGF14e$_{ox}$* lines) and silencing (*OsGF14e$_{si}$* lines) lines were analyzed. No significant difference was observed in the pollen viability and germination efficiency of the *OsGF14e$_{ox}$* lines as compared with the WT and VC lines while the *OsGF14e$_{si}$* lines displayed severe pollen sterility. (A) **P**ollen viability by I_2-KI staining method, (B) pollen viability by FDA staining method, and (C) *in vitro* pollen germination assay. At least 500 pollen grains from each line were studied.

Supplementary Figure 22. Biochemical analyses of the *OsGF14e* overexpressing (*OsGF14eox* lines) and silencing (*OsGF14esi* lines) transgenic rice lines in response to salinity stress. (A) Proline content, (B) glycine betaine content, (C) H_2O_2 content, (D) MDA content, (E) sodium (Na^+) content, and (F) potassium (K^+) content. Three independent transgenic lines (T_0) were considered in each case and results were represented as mean ± SEM. Statistical difference between the WT, VC, and transgenic lines was denoted by different letters at P<0.01 (b), P<0.001 (c) and P<0.0001 (d).

Supplementary Figure 23. Yeast one-hybrid assay for the interaction of *Os*GF14e with the *OsEG45* promoter. No interaction was observed. The interaction of p53 protein with pAbAi was used as a positive control. The interaction of *Os*GF14e with pAbAi was used as a negative control.

References

Achard, P., Cheng, H., De Grauwe, L., Decat, J., Schoutteten, H., and Moritz, T. (2006). Integration of plant responses to environmentally activated phytohormonal signals. Science. **311** 91–94.

Amirjani, M.R. (2012). Effect of NaCl stress on rice physiological properties. Archives Phytopath. Plant Protect.**45:** 228-243.

Aya, K., Ueguchi-Tanaka, M., Kondo, M., Hamada, K., Yano, K., Nishimura, M., and Matsuoka, M. (2009). Gibberellin modulates anther development in rice via the transcriptional regulation of GAMYB. Plant Cell. **21:** 1453–1472.

Benjamin, J.A., and Fernandez, D.E. (2009).MIKC* MADS-domain heterodimers are required for pollen maturation and tube growth in Arabidopsis. Plant Physiol. 149(4): 1713-1723.

Boavida, L.C., and McCormick, S. (2007). TECHNICAL ADVANCE: Temperature as a determinant factor for increased and reproducible in vitro pollen germination in Arabidopsis thaliana. Plant J.**52:** 570–582.

Bradford, M.M. (1976). A rapid and sensitive for the quantitation of microgram quantitites of protein utilizing the principle of protein-dye binding. Anal. Biochem *72:* 248-254.

Cao, W.H., Liu, J., He, X.J., Mu, R.L., Zhou, H.L.,Chen, S.Y., Zhang, J.S. (2007). Modulation of ethylene responses affects plant salt-stress responses. Plant Physiol. 143: 707-719

Carpentier, S., Witters, E., Laukens, K., Onckelen, H.V., Swennen, R., and Panis, B. (2007). Banana (Musa spp.) as a model to study the meristem proteome: Acclimation to osmotic stress. Proteomics **7:** 92-105.

Chen, C.Y., Wong, E.I., Vidali, L., Estavillo, A., Hepler, P.K., Wu, H.M. and Cheung, A.Y. (2002). The regulation of actin organization by actin-depolymerizing factor in elongating pollen tubes. Plant cell **14:** 2175– 2190.

Chen, F., Li, Q., Sun, L., and He, Z. (2006). The rice 14-3-3 gene family and its involvement in responses to biotic and abiotic stress. DNA Res. **13:** 53–63.

Chen, Y.S., David Ho, T.H., Liu, L., Lee, D.H., Lee, C.H., Chen, Y. R., Lin, S. Y., Lu, C.A., and Yu, S.M. (2019).Sugar starvation-regulated MYBS2 and 14-3-3 protein interactions enhance plant growth, stress tolerance, and grain weight in rice.Proc. Natl Acad. Sci. USA. **116(43):** 21925–21935.

Chhun, T., Aya, K., Asano, K., Yamamoto, E., Morinaka, Y., Watan, M., Kitano, H., Ashikari, M., Matsuoka, M., and Ueguchi-Tanaka, M. (2007). Gibberellin Regulates Pollen Viability and Pollen Tube Growth in Rice. Plant cell.**19:**3876-3888.

Ciopraga, J., Gozia, O., Tudor, R., Brezuica, L., and Doyle, R.J. (1999). Fusarium sp growth inhibition by wheat germ agglutinin. Biochim. Biophys. Acta. **1428 (2):** 424-432.

Clough, S.J., and Bent, A.F. (1998). Floral dip: a simplified method for *Agrobacterium*-mediated transformation of *Arabidopsis thaliana*. Plant J.**16:** 735–743.

Cooper, B., Clarke, J., Budworth, P., Kreps, J., Hutchison, D., Park, S., Guimil, S., Dunn, M., Luginbuhl, P., Ellero, C., Goff, S.A., and Glazebrook, J. (2003). A network of rice genes associated with stress response and seed development. Proc. Natl Acad. Sci. USA.**100:** 4945-4950.

Cummings, R.D., and Etzler, M.E. (2009). R-type Lectins. Essentials of Glycobiology. **2nd** edition. Chapter 28.

Damico, D.C.S., Freire, M.G.M., Gomes, V.M., Toyama, M.H., Marangoni, S., Novello, J.C., and Macedo, L. (2003). Isolation and Characterization of a Lectin from Annona muricataSeeds. J Protein Chem. **22:** 655-661.

Datta, K., Koukolikova-Nicola, Z., Baisakh, N., Oliva, N., and Datta, S.K. (2000). Agrobacterium-mediated engineering for sheath blight resistance of indica rice cultivars from different ecosystems. Theor. Appl. Genet.**100 (6):** 832-839.

Datta, R., Chamusco, K.C., and Chourey, P.S. (2002). Starch biosynthesis during pollen maturation is associated with altered patterns of gene expression in maize. Plant Physiol. **130 (4):** 1645-1656.

Datta, R., Kumar, D., Sultana, A., Hazra, S., Bhattacharyya, D., and Chattopadhyay, S. (2015). Glutathione regulates ACC synthase transcription via WRKY33 and ACC oxidase by modulating mRNA stability to induce ethylene synthesis during stress. Plant Physiol. **169:** 2963-2981.

Datta, R., Sahid, S., Paul, S. (2020) Networking by small molecule hormones during drought stress in plants. In: Khan MIR, Singh A, Poór P, eds. Improving abiotic stress tolerance in plants. Boca Raton: CRC Press, 203–228

Daugherty, C.J., Rooney, M.F., Miller, P.W., and Ferl, R. J. (1996). Molecular organization and tissue-specific expression of an Arabidopsis 14-3-3 gene. Plant Cell **8:** 1239-1248.

Freire, M.G.M., Gomes, V.M., Corsini, R.E., De Simone, S.G., Novello, J.C., Marangoni, S., and Macedo, L. (2002). Isolation and partial characterization of novel lectin from Talisiaesculenta seeds that interferes with fungal growth. Plant Physiol. Biochem. **40(1):**61-68.

Gall, L.H., Philippe, F., Domon, J.M., Gillet, F., Pelloux, J., and Rayon, C. (2015). Cell wall metabolism in response to abiotic stress. Plants **4:**112–166.

Ganguly, M., Datta, K., Roychoudhury,A., Gayen, D., Sengupta, D.N., and Datta, S.K. (2012). Overexpression of Rab16A gene in indica rice variety for generating enhanced salt tolerance. Plant Signal Behav. **7(4):** 502-509.

García-Cano, E., Zaltsman, A., and Citovsky, V. (2014). Assaying proteasomal degradation in a cell-free system in plants. J Vis Exp. **85:**e51293.

Golldack, D., Li, C., Mohan, H., Probst, N. (2014) Tolerance to drought and salt stress in plants unravelling the signalling networks. Front in plant sci. **5:**151.

Goto, N., and Pharis, R.P. (1999). Role of gibberellins in the development of floral organs of gibberellin-deficient mutant, *ga1-1*, of *Arabidopsis thaliana*. Can. J. Bot. **77**: 944-954.

Grieve, C.M., and Grattan, S. R. (1983). Rapid assay for the determination of water soluble quaternary ammonium compounds. Plant Soil **70:** 303-307.

Guo, W., Zhao, J., Li, X., Qin, L., Yan, X., and Liao, H. (2011). A soybean β-expansin gene GmEXPB2 intrinsically involved in root system architecture responses to abiotic stresses. Plant J. **66(3):**541-552.

Han, Y., Li, Ax., Li, F., Zhao, Mr., and Wang, W. (2012). Characterization of a wheat (Triticumaestivum L.) expansin gene, TaEXPB23, involved in the abiotic stress response and phytohormoneregulation. Plant Physiol Biochem. **54:** 49-58.

He, X., Li, L., Xu, H., Xi, J., Cao, X., Xu, H., Rong, S., Dong, Y., Wang, C., and Chen, R. (2016). OsJRL, a rice jacalin-related mannose-binding lectin gene, enhances *Escherichia coli* viability under high-salinity stress and improves salinity tolerance of rice. Plant Biol.**19:** 257-267.

Hirano, K., Teraoka, T., Yamanaka, H., Harashima, A., Kunisaki, A., Takahashi, H., and Hosokawa, D. (2000). Novel Mannose-binding rice lectin composed of some isolectins and its relation to a stress-inducible salT gene. Plant Cell Physiol. **41(3):** 258-267.

Jefferson, R.A., Kavangh T.A., Bevan M.W. (1987). Gus fusions: β-glucuronidase as a sensitive and versatile gene fusion marker in higher plants. EMBO J. **6**:3901-3907.

Jiang, S., Chen, Y., Wang, M., Yin, A., Pan, Y., Gu, B., Yu, G., Li, Y., Wong, B.H.C., Liang, Y., and Sun, H. (2012a). A novel lectin from *Agrocybeaegerita* shows high binding selectivity for terminal *N*-acetylglucosamine. Biochem J. **443 (2):** 369-378.

Jiang, S.S., Liang, X.N., Li, X., Wang, S.L., Lv, D.W., Ma, C.Y., Li, X.H., Ma, W.J., and Yan, Y.M. (2012b). Wheat drought-responsive grain proteome analysis by linear and nonlinear 2-DE and MALDI-TOF mass spectrometry. Int. J Mol. Sci. **13:** 16065-16083.

Jiang, S.Y., Ma,Z., and Ramachandran, S. (2010). Evolutionary history and stress regulation of the lectin superfamily in higher plants. BMC Evol. Biol. **10:** 79.

Kurniasih, B., Greenway, H., and Colmer, T.D. (2013). Tolerance of submerged germinating rice to 50-200mM NaCl in aerated solution. Physiol. Plant. **149:** 222-233.

Lannoo, N., and Van Damme, E.J.M. (2014) Lectin domains at the frontiers of plant defense Front. Plant Sci. **5:** 397.

Li, F., Han, Y.Y., Feng, Y. A., Xing, S. C., Zhao, M. R., Chen, Y.H., and Wang, W. (2013). Expression of wheat expansin driven by the RD29 promoter in tobacco confers water stress tolerance without impacting growth and development. J. Biotechnol. **163:** 281– 291.

Li, G., Yang, X., Zhang, X., Song, Y., Liang, W., Zhang, D. (2018). Rice Morphology Determinant-Mediated Actin Filament Organization Contributes to Pollen Tube Growth. Plant. Physiol. **177:** 255-270.

Lichtenthaler, H. K. (1987). Chlorophylls and carotenoids, the pigments of photosynthetic biomembranes. Methods Enzymol.**148:** 350–382.

Liu, B., Zhao, S., Li, P., Yin, Y., Niu, Q., Yan, J., Huang, D. (2021). Plant buffering against the high-light stress-induced accumulation of CsGA2ox8 transcripts via alternative splicing to finely tune gibberellins levels and maintain hypocotyls elongation. Horticulture Res. **8.2**.

Liu, Q., Yang, J., Zhang, S., Zhao, J., Feng, A., Yang, T., Wang, X., Mao, X., Dong, J., Zhu, X., Leung, H., Leach, J.E., and Liu, B. (2015). *OsGF14e* positively regulates panicle blast resistance in rice. Biochem. Biophys. Res. Commun. **471:** 247–252.

Liu, Q., Yang, J., Zhang, S., Zhao. J., Feng, A., Yang, T., Wang, X., Mao, X., Dong, J., Zhu, X., Leung, H., Leach, J.E., and Liu, B. (2016).*OsGF14b* positively regulates panicle blast resistance but negatively regulates leaf blast resistance in Rice. Mol Plant-Microbe Interact. **29:** 46–56.

Lo, S.F., Yang, S.Y., Chen, K.T., Hsing, Y.L., Zeevaart, J.A.D., Chen, L.J., and Yu, S.M. (2008).A Novel Class of Gibberellin 2-Oxidases Control Semi dwarfism, Tillering, and Root Development in Rice. Plant Cell **20:** 2603-2618.

Lü, P., Kang, M., Jiang, X., Dai, F., Gao, J., and Zhang, C. (2013). RhEXPA4, a rose expansin gene, modulates leaf growth and confers drought and salt tolerance to Arabidopsis. Planta. **237(6):**1547-1559.

Ludidi, N., Heazlewood, J. L., Seoighe, C., Irving, H. R., and Gehring, C. (2002). Expansin-Like Molecules: Novel Functions Derived from Common Domains. J. Mol. Evol. **54(5):** 587-594.

Ma, N.L., Lah, W.A.C., Kadir, N.A., Mustaqim, M., Rahmat, Z., Ahmad, A., Lam, S.D., Ismail, M.R. (2018). Susceptibility and tolerance of rice crop to salt threat: Physiological and metabolic inspections. PLoS One **13 (2)**: 0192732.

Manosalva, P.M., Bruce, M., and Leach, J.E. (2011). Rice 14□3□3 protein (GF14e) negatively affects cell death and disease resistance. Plant J. **68:** 777-787.

Miyakawa, T., Hatani, K.I., Miyauchi, Y., Suwa, Y.I., Sawano, Y., and Tanokura, M. (2014). Secreted protein with plant-specific cysteine-rich motif functions as a mannose-binding lectin that exhibits antifungal activity. Plant Physiol. **166:** 766-778.

Moons, A., Bauw, G., Prinsen, E., Van Montagu, M., and Van Der Straeten, D. (1995). Molecular and physiological responses to abscisic acid and salts in roots of salt-sensitive and salt-tolerant Indica rice varieties. Plant Physiol. **107:**177-186.

Moons, A., Gielen, J., Vandekerckhove, J., Van Der Straeten, D., Gheysen, G., and Van Montagu, M. (1997). An abscisic-acid-and salt-stress-responsive rice cDNA from a novel plant gene family. Planta. **202:** 443-454.

Muhlemann, J. K., Younts, T. L. B., and Muday, G. K. (2018). Flavonols control pollen tube growth and integrity by regulating ROS homeostasis during hightemperature stress. Proc. Natl Acad. Sci. USA. **115**: E11188–E11197.

Munns, R. (2002). Comparative physiology of salt and water stress. Plant Cell Environ. **25:** 239-250.

Muthamilarasan, M., and Prasad, M. (2013). Plant innate immunity: an updated insight into defense mechanism. J. Biosci. **38:** 433–449.

Nublat, A., Desplans, J., Casse, F., and Berthomieu, P. (2001). *Sas1*, an Arabidopsis mutant overaccumulating sodium in the shoot, shows deficiency in the control of the root radial transport of sodium. Plant Cell. **13**: 125-137.

Paul, S., Ali, N., Datta, S.K., and Datta, K. (2014). Development of an iron-enriched High-yieldings Indica rice cultivar by introgression of a high-iron trait from transgenic iron-biofortified rice. Plant Foods Hum Nutr. **69**: 203-208.

Paul, S., Gayen, D., Datta, S.K., Datta, K. (2015). Dissecting root proteome of transgenic rice cultivars unravels metabolic alterations and accumulation of novel stress responsive proteins under drought stress. Plant Sci. **234:** 133–143.

Plaza-Wüthrich, S., Blösch, R., Rindisbacher, A., et al (2016) Gibberellin deficiency confers both lodging and drought tolerance in small cereals, Front. Plant Sci **7**:643.

Qin, F., Kodaira, K.S., Maruyama, K., et al. (2011) SPINDLY, a negative regulator of gibberellic acid signaling, is involved in the plant abiotic stress response. Plant Physiol **157**:1900–1913.

Sahid, S., Roy, C., Paul, S., and Datta, R. (2020). Rice lectin protein r40c1 imparts drought tolerance by modulating S-adenosylmethionine synthase 2, stress-associated protein 8 and chromatin-associated proteins. J. Exp. Bot. **71 (22)**: 7331-7346.

Schmidt, R., Schippers, J. H. M., Mieulet, D., Watanabe, M., Hoefgen, R., Guiderdoni, E., and Mueller- Roeber, B. (2014).SALT-RESPONSIVE ERF1 Is a Negative Regulator of Grain Filling and Gibberellin-Mediated Seedling Establishment in Rice. Mol. Plant **7(2):** 404-421.

Schofta, V.K., Chumaka, N., Choib, Y., Hannonc, M., Gracia-Aguilara, M., Machlicovaa, A., Slusarza, L., Mosioleka, M., Parkb, J.S., Parkb, G.T., Fischerc, R.L., and Tamarua, H. (2011). Function of the DEMETER DNA glycosylase in the Arabidopsis thaliana male gametophyte. Proc. Natl Acad. Sci. USA. **108(19):** 8042-8047.

Schultz, T.F., Medina, J., Hill, A., and Quatrano, R.S. (1998).14-3-3 proteins are part of an abscisic acid-VIVIPAROUS1 (VP1) response complex in the Em promoter and interact with VP1 and EmBP1. Plant cell **10:** 837-847.

Sehnke, P.C., Laughner, B., Cardasis, H., Powell, D., and Ferl, R.J. (2006). Exposed loop domains of complexed 14-3-3 proteins contribute to structural diversity and functional specificity. Plant Physiol. **140:** 647–660.

Shahidi-Noghabi, S., Van Damme, E.J.M., and Smagghe, G. (2009). Carbohydrate-binding activity of the type-2 ribosome-inactivating protein SNA-I from Elderberry (SambucusNigra) is a determining factor for its insecticidal activity. Phytochem. **69:** 2972- 2978.

Shahidi□Noghabi, S., Van Damme, E.J.M., and Smagghe, G. (2009). Expression of Sambucusnigra agglutinin (SNA□I′) from elderberry bark in transgenic tobacco plants results in enhanced resistance to different insect species. Transgenic Res. **18:** 249– 259.

Shehab, G. G., Ahmed, O. K., and El-Beltagi, H. S. (2010). Effects of various chemical agents for alleviation of drought stress in rice plants (*Oryza sativa* L.). Notulae Botanicae Horti Agrobotanici Cluj-Napoca **38**: 139–48.

Shen, Q., Zhan, X., Yang, P., Li, J., Chen, J., Tang, B., Wang, X., and Hong, Y. (2019). Dual Activities of Plant cGMP-Dependent Protein Kinase and Its Roles in Gibberellin Signaling and Salt Stress. Plant cell **31:** 3073-3091.

Simossis, V.A., and Heringa, J. (2005). PRALINE: A multiple sequence alignment toolbox that integrates homology-extended and secondary structure information. Nucleic Acids Res. **W33:** W289-294.

Singh, P., and Zimmerli, L. (2013).Lectin receptor kinases in plant innate immunity. Front Plant Sci.**4:** 124.

Song, M., Xu, W., Xiang, Y., Jia, H., Zhang, L., and Ma, Z. (2014). Association of jacalin-related lectins with wheat responses to stresses revealed by transcriptional profiling. Plant Mol. Biol. **84:** 95-110.

Spadoro-Tank, J.P., and Etzler, M.E. (1988).Heath Shock Enhances the Synthesis of a Lectin-Related Protein in Dolichosbiflorus Cell Suspension Cultures. Plant Physiol. **88:** 1131-1135.

Ueguchi-Tanaka, M., Nakajima, M., Katoh, E., Ohmiya, H., Asano, K., Saji, S., Hongyu, X., Ashikari, M., Kitano, H., Yamaguchi, I., and Matsuoka, M. (2007). Molecular interactions of a soluble gibberellin receptor, GID1, with a rice DELLA protein, SLR1 and gibberellin. Plant Cell **19:** 2140–2155.

Van Damme, E.J.M., Hao, Q., Chen, Y., Barre, A., Vandenbussche, F., and Desmyter, S. (2001). Ribosome-inactivating proteins: a family of plant proteins that do more than inactivate ribosomes. Crit. Rev. Plant Sci. **20:**395–465.

Van Damme, Els., Lannoo, N., and Peumans, W. (2008). Plant lectins. Adv Bot Res. **48:**107-209.

Van Hove, J., Jaeger, G.D., Winne, N.D., Guisez, Y., Van Damme, E.J.M. (2015). The Arabidopsis lectin EULS3 is involved in stomatal closure. Plant Sci. **238**: 312-322.

Van Hove, J., Stefanowicz, K., De Schutter, K., Eggermont, L., Lannoo, N., Al Atalah, B., Van Damme, E.J.M. (2014) Transcriptional profiling of the lectin ArathEULS3 from *Arabidopsis thaliana* toward abiotic stresses. J Plant Physiol. **171**:1763–1773.

Vandenbussche, F., Desmyter, S., Ciani, M., Proost, P., Peumans, W.J., and Van Damme E.J.M. (2004a).Analysis of the in planta antiviral activity of elderberry ribosome-inactivating proteins. Eur. J. Biochem. **271:**1508–1515.

Vandenbussche, F., Desmyter, S., Ciani, M., Proost, P., Peumans, W.J., and Van Damme E.J.M. (2004b).The type1 and type 2 ribozome inactivating proteins from Iris confer transgenic tobacco plants local but not systemic protection against viruses. Planta. **220:** 211-221.

Verma, V., Ravindran, P., Kumar, P.P. (2016). Plant-hormone mediated regulation of stress responses. BMC Plant Biol. **16**:86.

Waadt, R., Schmidt, L. K., Lohse, M., Hashimoto, K., Bock, R., and Kudla, J. (2008). Multicolor bimolecular fluorescence complementation reveals simultaneous formation of alternative CBL/CIPK complexes in planta. Plant J. **56:**505-516.

Woodrow, P., Ciarmiello, L.F., Annunziata, M.G., Pacifico, S., Iannuzzi, F., Mirto, A., D'Amelia, L., Dell'Aversana, E., Piccolella, S., Fuggi, A., and Carillo, P. (2016). Durum wheat seedling responses to simultaneous high light and salinity involve a fine reconfiguration of amino acids and carbohydrate metabolism. Physiol. Plant. **159:** 290-312.

Wu, Y., Thorne, E.T., Sharp, R.E., and Cosgrove, D.J. (2001). Modification of expansin transcript levels in the maize primary root at low water potentials. Plant Physiol. **126(4):**1471-1509.

Yan, P., Shen, W., Gao, X.Z., Li, X., Zhou, P., and Duan, J. (2012) High-Throughput Construction of Intron-Containing Hairpin RNA Vectors for RNAi in Plants. Plos One. **7(5):** e38186. doi:10.1371/journal.pone.0038186.

Yang, G.X., Jan, A., Shen, S.H., Yazaki, J., Ishikawa, M., Shimatani, Z., Kishimoto, N., Kikuchi, S., Matsumoto, H., and Komatsu, S. (2004). Microarray analysis of brassinosteroids- and gibberellin-regulated gene expression in rice seedlings. Mol Gen Genomics. 271: 468-478.

Yang, Z.P., Li, H.L., Guo, D., Tang, X., and Peng, S.Q. (2014). Identification and characterization of the 14-3-3 gene family in Heveabrasiliensis. Plant Physiol and Biochem. **80:** 121-127.

Yin, L., Wang, S., Eltayeb, A.E., Uddin, M.I., Yamamoto, Y., and Tsuji, W. (2010). Overexpression of dehydroascorbate reductase, but not monodehydroascorbate reductase, confers tolerance to aluminum stress in transgenic tobacco. Planta. **231:** 609–621.

Yin, W., Xiao, Y., Niu, M., Meng, W., Li, L., Zhang, X., Liu, D., Zhang, G., Qian, Y., Sun, Z., Huang, R., Wang, S., Liu, C.M., Chu, C., Tong, H. (2020). ARGONAUTE2 enhances grain length and salt tolerance by activating BIG GRAIN 3 to modulate cytokinin distribution in rice. Plant Cell. **32**: 2292-2306.

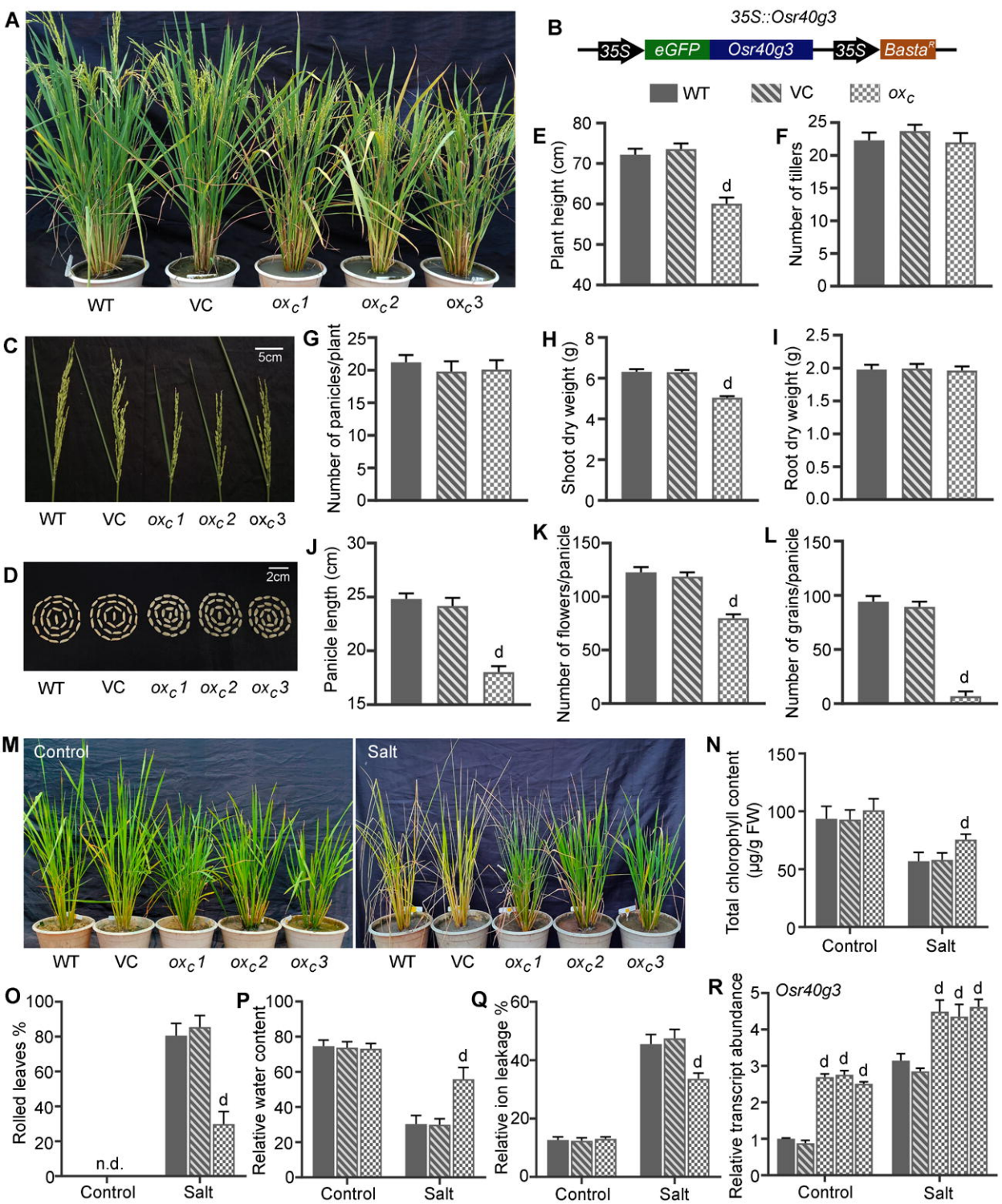
A
WT
VC
oxc1
oxc2
oxc3
B
35S::Osr40g3
35S
eGFP
Osr40g3
35S
Basta^R
WT
VC
oxc
C
5cm
D
2cm
E
Plant height (cm)
F
Number of tillers
G
Number of panicles/plant
H
Shoot dry weight (g)
I
Root dry weight (g)
J
Panicle length (cm)
K
Number of flowers/panicle
L
Number of grains/panicle
M
Control
Salt
N
Total chlorophyll content (μg/g FW)
O
Rolled leaves %
n.d.
P
Relative water content
Q
Relative ion leakage %
R
Osr40g3
Relative transcript abundance
Control
Salt

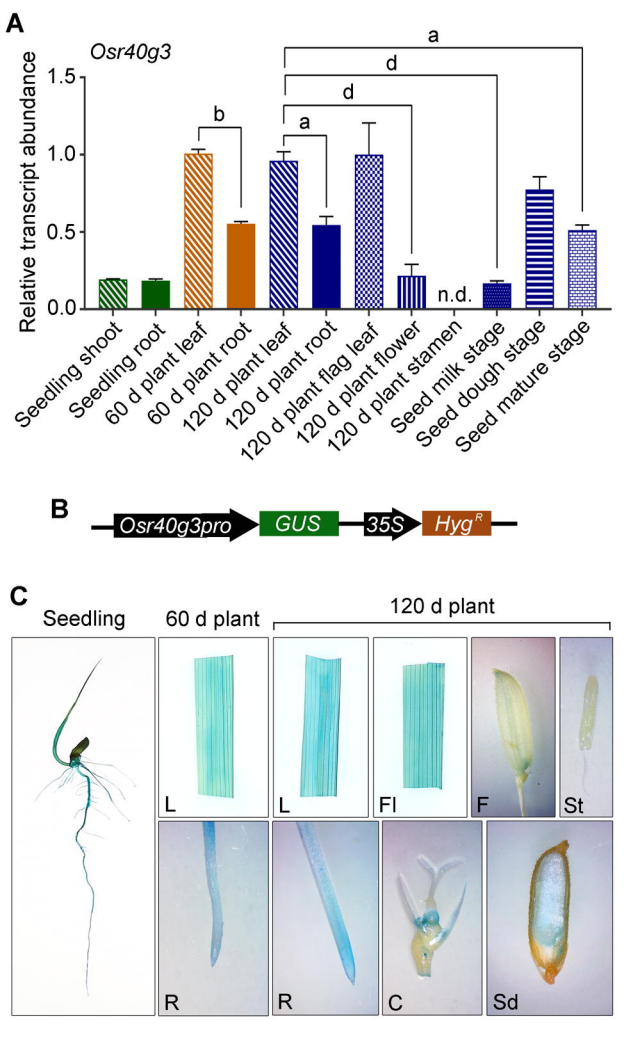
A
Osr40g3
Relative transcript abundance
1.5
1.0
0.5
0.0
a
d
d
b
a
n.d.
Seedling shoot
Seedling root
60 d plant leaf
60 d plant root
120 d plant leaf
120 d plant root
120 d plant flag leaf
120 d plant flower
120 d plant stamen
Seed milk stage
Seed dough stage
Seed mature stage
B
Osr40g3pro
GUS
35S
Hyg^R
C
Seedling
60 d plant
120 d plant
L
L
Fl
F
St
R
R
C
Sd

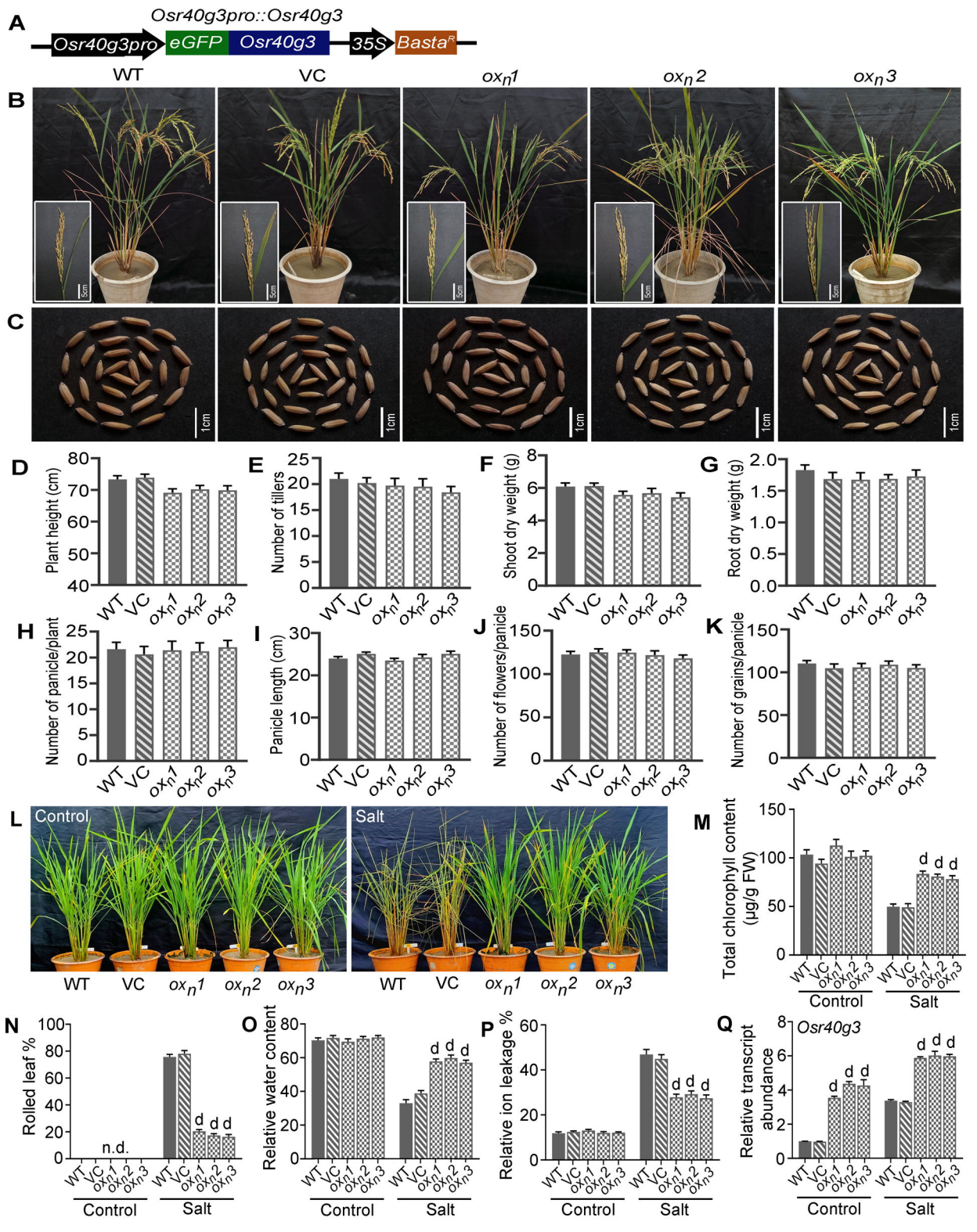
A
Osr40g3pro::Osr40g3
Osr40g3pro
eGFP
Osr40g3
35S
Basta^R
WT
VC
oxn1
oxn2
oxn3
B
5cm
C
1cm
D
Plant height (cm)
E
Number of tillers
F
Shoot dry weight (g)
G
Root dry weight (g)
H
Number of panicle/plant
I
Panicle length (cm)
J
Number of flowers/panicle
K
Number of grains/panicle
L
Control
Salt
M
Total chlorophyll content (μg/g FW)
N
Rolled leaf %
n.d.
O
Relative water content
P
Relative ion leakage %
Q
Osr40g3
Relative transcript abundance
Control
Salt

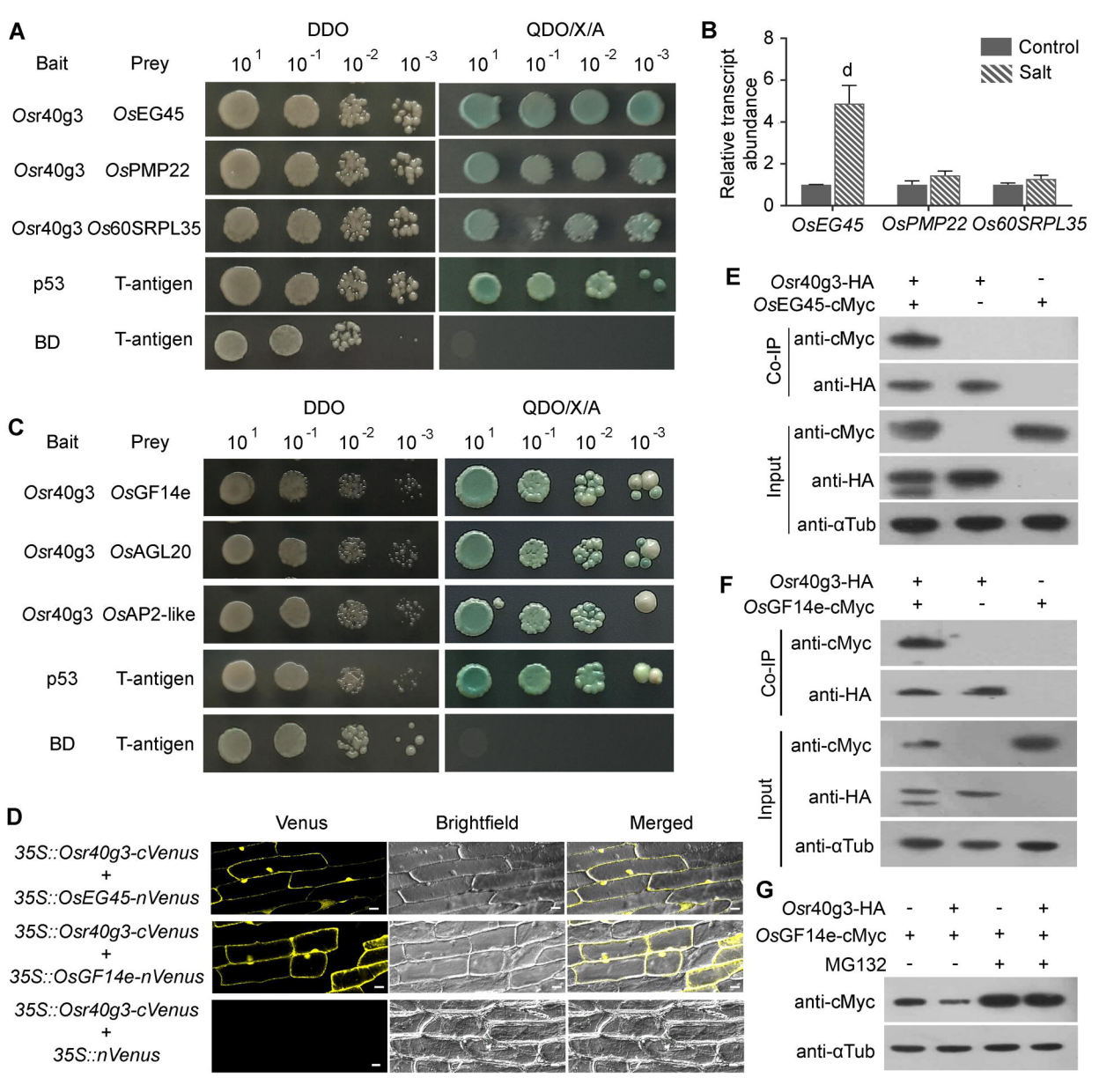
A
DDO
QDO/X/A
Bait
Prey
10 1
10 -1
10 -2
10 -3
Osr40g3
OsEG45
Osr40g3
OsPMP22
Osr40g3
Os60SRPL35
p53
T-antigen
BD
T-antigen
B
Relative transcript abundance
Control
Salt
d
OsEG45
OsPMP22
Os60SRPL35
C
DDO
QDO/X/A
Bait
Prey
Osr40g3
OsGF14e
Osr40g3
OsAGL20
Osr40g3
OsAP2-like
p53
T-antigen
BD
T-antigen
D
Venus
Brightfield
Merged
35S::Osr40g3-cVenus
+
35S::OsEG45-nVenus
35S::Osr40g3-cVenus
+
35S::OsGF14e-nVenus
35S::Osr40g3-cVenus
+
35S::nVenus
E
Osr40g3-HA
OsEG45-cMyc
Co-IP
anti-cMyc
anti-HA
Input
anti-cMyc
anti-HA
anti-αTub
F
Osr40g3-HA
OsGF14e-cMyc
Co-IP
anti-cMyc
anti-HA
Input
anti-cMyc
anti-HA
anti-αTub
G
Osr40g3-HA
OsGF14e-cMyc
MG132
anti-cMyc
anti-αTub

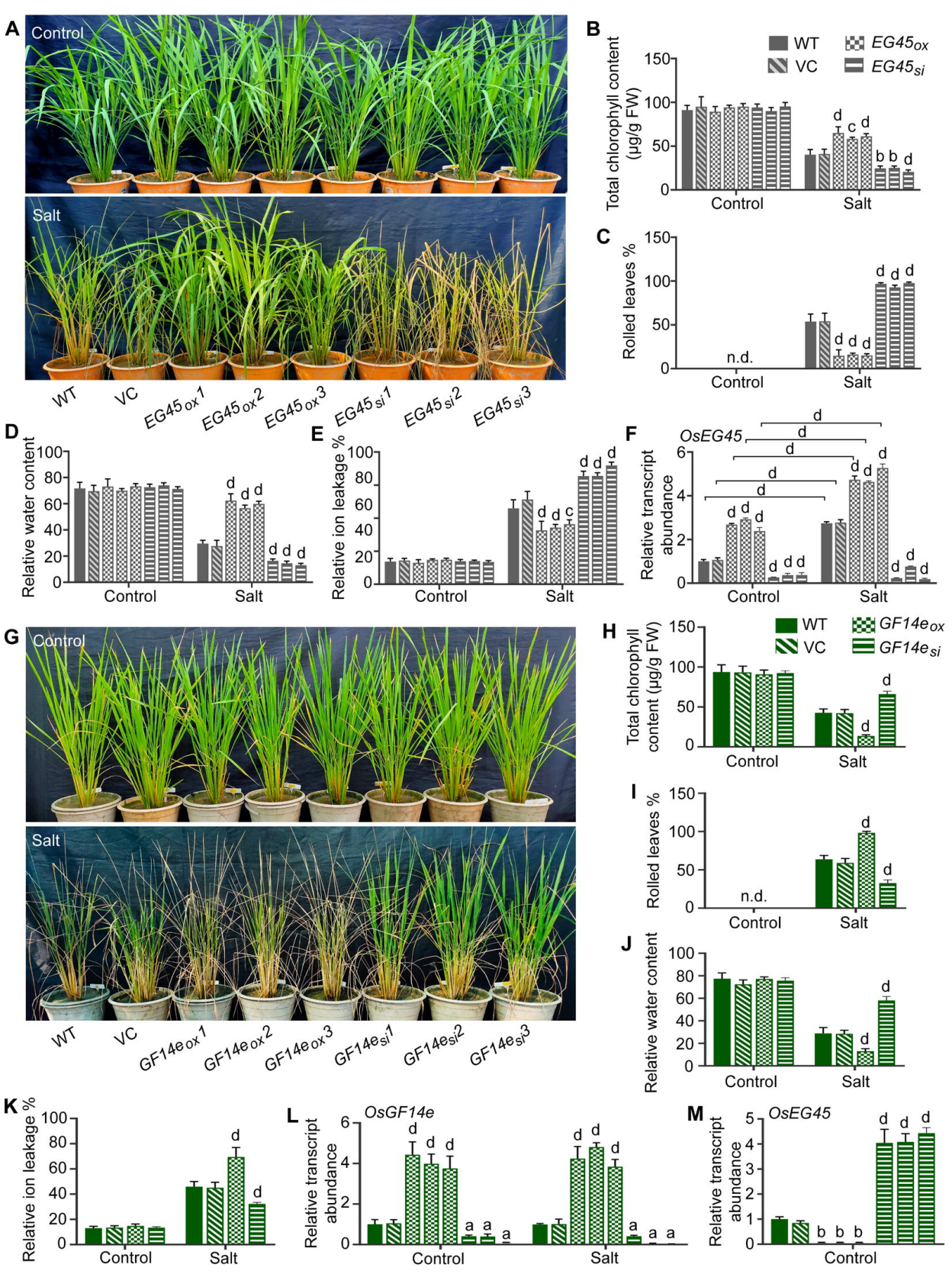
A
Control
Salt
WT
VC
EG45 ox 1
EG45 ox 2
EG45 ox 3
EG45 si 1
EG45 si 2
EG45 si 3
B
WT
VC
EG45ox
EG45si
Total chlorophyll content (μg/g FW)
Control
Salt
C
Rolled leaves %
n.d.
D
Relative water content
E
Relative ion leakage %
F
OsEG45
Relative transcript abundance
G
H
GF14eox
GF14esi
I
J
K
L
OsGF14e
M
OsEG45

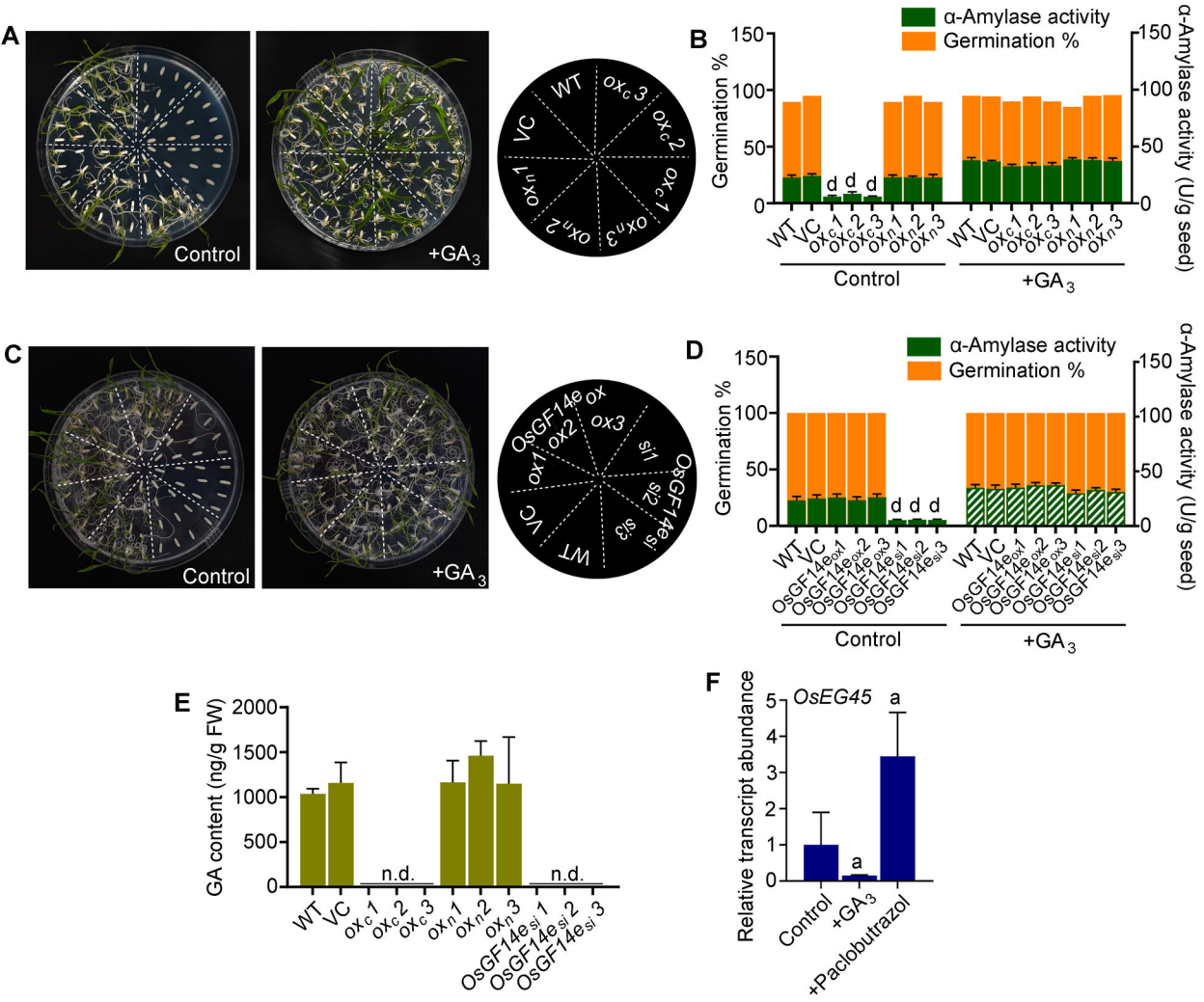
A
Control
+GA3
WT
oxc 3
oxc 2
oxc 1
oxn 3
oxn 2
oxn 1
VC
B
α-Amylase activity
Germination %
Germination %
α-Amylase activity (U/g seed)
d d d
WT VC oxc1 oxc2 oxc3 oxn1 oxn2 oxn3 WT VC oxc1 oxc2 oxc3 oxn1 oxn2 oxn3
Control
+GA3
C
Control
+GA3
OsGF14e ox
ox1 ox2
ox3
si1
OsGF14e si2
si3
WT
VC
D
α-Amylase activity
Germination %
Germination %
α-Amylase activity (U/g seed)
d d d
WT VC OsGF14eox1 OsGF14eox2 OsGF14eox3 OsGF14esi1 OsGF14esi2 OsGF14esi3 WT VC OsGF14eox1 OsGF14eox2 OsGF14eox3 OsGF14esi1 OsGF14esi2 OsGF14esi3
Control
+GA3
E
GA content (ng/g FW)
n.d.
n.d.
WT VC oxc1 oxc2 oxc3 oxn1 oxn2 oxn3 OsGF14esi1 OsGF14esi2 OsGF14esi3
F
OsEG45
Relative transcript abundance
a
a
Control
+GA3
+Paclobutrazol

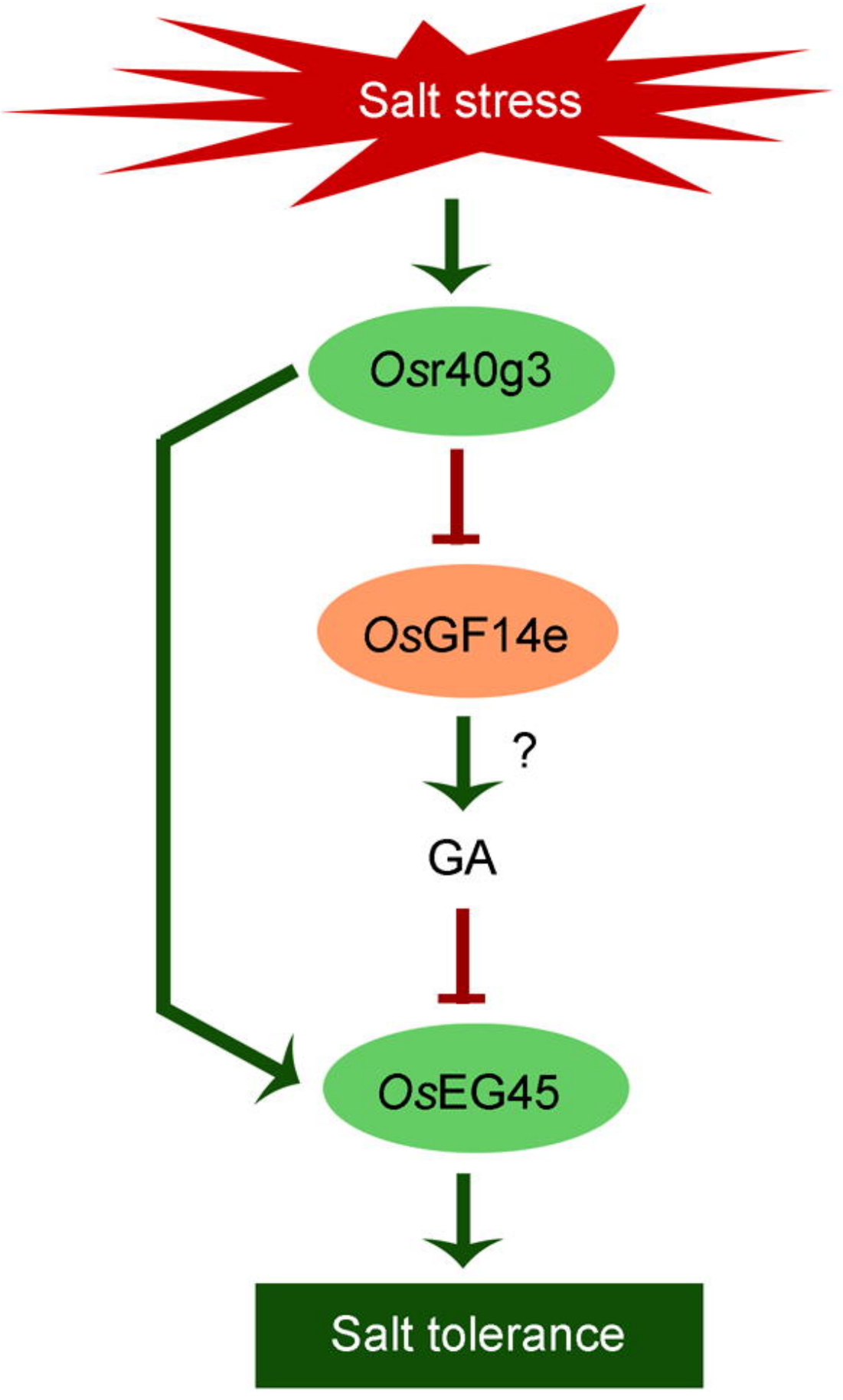
Salt stress
Osr40g3
OsGF14e
?
GA
OsEG45
Salt tolerance